ACTIVATION OF LOCUS COERULEUS AND CONCURRENT
OBSERVATION OF PERFORANT PATH EVOKED POTENTIAL,
SINGLE UNIT ACTIVITY AND EEG IN THE DENTATE
GYRUS OF THE RAT

CORDELL GODFREY CLARKE

Activation of Locus Coeruleus and Concurrent Observation
of Perforant Path Evoked Potential, Single Unit Activity
and EEG in the Dentate Gyrus of the Rat.

By

©Cordell Godfrey Clarke

A Thesis Submitted to the School of Graduate
Studies in Partial Fulfillment of the
Requirements for the Degree of
Master of Science

Department of Basic Sciences
Faculty of Medicine
Memorial University of Newfoundland
May 1995

St. Johns   Newfoundland

ABSTRACT

Glutamate ejection in the vicinity of locus coeruleus (LC) in urethane anesthetized rats was used to selectively activate norepinephrine (NE) release from LC fibers. Extracellular units, 0.1 Hz perforant path-evoked potentials (PP-EP), and hippocampal EEG were concurrently monitored in the dentate gyrus. In all experiments, LC activation induced potentiation of the PP-EP. Significant potentiation of the PP-EP was not seen until an average of 20 s. after glutamate ejection. Significant changes in spontaneous neuronal activity occurred both immediately and with a delay following LC activation. Subgranular layer, nonbursting neurons with narrow action potentials were immediately excited by NE for an average duration of 26.6 s. Distal subgranular layer, nonbursting neurons with wider action potentials were inhibited by LC activation for an average duration of 88 s. Bursting hilar neurons showed a delayed suppression, beginning an average of 10 s. after the flag and lasting for an average of 276 s. Finally, a group of three cells were unaffected. Theta was present before and after the ejection in the majority of experiments (11) and increases in theta frequency were seen in 3 animals. A loss of theta occurred within an average of 36 s. after the ejection in 8 experiments and lasted an average of 6 min.

Based on the electrophysiological and anatomical results, a model is suggested

in which there are three different interneuron types which are affected differently by LC-NE (excitation, inhibition, and unaffected) and contribute to modulating excitation and inhibition in the system. Bursting cells are either unaffected or show prolonged reduced activity similar to the period of LC suppression.

It seems that conditions are set up by LC-NE release which contribute to the promotion of an increased coupling between PP input and granule cell output which would increase DG circuit throughput.

ACKNOWLEDGEMENTS

TABLE OF CONTENTS

LIST OF FIGURES

LIST OF TABLES

INTRODUCTION

This study assesses the effects of synaptically released norepinephrine (NE) on the dentate gyrus (DG) of the rat hippocampus by using glutamatergic stimulation of the locus coeruleus (LC). Three electrophysiological parameters are evaluated concurrently: single unit activity, the perforant path (PP) evoked potential (EP), and the EEG. There are a number of controversies inherent in the research performed to date on this topic. There is evidence to support both the excitation and inhibition of interneuron activity by NE applied to the DG and there is evidence to support the claim that NE affects EEG as well as evidence that it has no effect at all. However, numerous studies agree that NE causes an increase in the amplitude of the PP-EP. Two methodologies have previously been employed to assess NE effects at this site, electrical stimulation of the LC (e.g. Segal and Bloom, 1974), and directly applied NE (e.g. Neuman and Harley, 1983). Chemical stimulation of the LC had not been used until more recently (e.g. Harley and Milway, 1986).

<u>Dentate Gyrus organization and NE Input:</u>

<u>A:Dentate Gyrus Anatomy:</u>

The DG consists of a folded sheet of one main cell type, the granule cells
(10-15 μm), which are present in the granule cell layer (see fig. 1). There are
interneurons (20-40 μm) also located throughout most of the DG both interspersed in
the granule cell layer and located just below it. Finally, the polymorph region, or hilus,
is located between the two blades of the granule cell layer, consists of both
interneurons and quasi-principal pseudo-pyramidal cells (Amaral, 1978), and is shown in
figure #1 as zone 4. The granule cells send dendrites to the molecular layer of the
dentate, which is a zone consisting mainly of fibres. This area consists of three basic
layers, the inner molecular, middle molecular and outer molecular layers. The entorhinal
cortex provides the main cortical excitatory connections via the PP which synapses
with the dendrites of granule cells in the middle and outer molecular layer. The axons
of granule cells (mossy fibres) send connections to CA3 of the hippocampus proper,
while the interneurons control local inhibition and excitation in the system (see figure
#1).
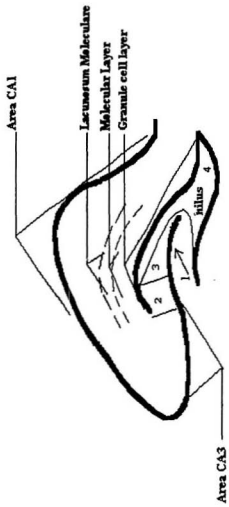
Figure #1: Diagram representing a transverse view of the hippocampus, showing pertinent cell layers. Connections are described in the text of the introduction. Zones 1-4 are those described by Amaral (1978).

Area CA1

Lacunosum Molecular
Molecular Layer
Granule cell layer

hilus

Area CA3

1 2 3 4

B: Sources of NE:

The sole supply of neuronal NE in the DG comes from a nucleus in the dorsal brain stem known as the LC. Pickel et al. (1974) initially reported that the densest projections from the LC end in the DG of the hippocampus and the central nucleus of the amygdala.

C: Synaptic Distribution: NE Terminals and Receptors:

Receptor Distribution:

Norepinephrine is a monoamine with two families of receptors present in the hippocampal formation, the α and β receptors. The α and β receptor families differ in their densities over the area of the hippocampus. Studies of the binding of radioactive ligands to these receptors and their subtypes followed by treatment with competitive agonists and antagonists for the subtypes have aided in the recognition of these subtypes and their distribution in brain tissue. Alexander et al (1975) using tritiated alprenolol, a β-adrenergic receptor antagonist, were the first to identify β-receptor binding in the rat CNS. They found the highest density of β-receptors in the hippocampus and limbic cortex.

4

Young and Kuhar (1980) used tritiated WB-4101 (selective for $\alpha 1$ adrenoceptors) and tritiated p-aminoclonidine (PAC)(selective for $\alpha 2$ adrenoceptors) to locate and differentiate fields of α-adrenergic receptors in the rat brain. They found high levels of $\alpha 1$-receptors in the molecular layer of the DG and also high levels in the caudal dentate. High levels of $\alpha 2$-receptors were seen in the LC.

Tiong and Richardson (1990) using iodocyanopindolol tagged with ^{125}I assessed the fields of β-adrenoceptors in rat amygdala and hippocampus. They also used other antagonists which were selective to the $\beta 1$ and $\beta 2$ subtypes to distinguish between them. The results indicated that 70% of the receptors in the hippocampus were $\beta 1$ and the other 30% were $\beta 2$.

Terminal Distribution:

Koda et al. (1977 & 1978) used both light microscopy to visualize glyoxylic acid induced fluorescent (GIF) varicosities and electron microscopy to visualize small granular vesicles (SGV) in the DG. They found a cut to the dorsal tegmental bundle (DTB), in which the LC fibres run, depletes the supply of catecholamines to the hippocampus. Both the GIF varicosities and the SGV vesicles were decreased in

5

number in the dentate hilus. The decrease was greatest ipsilateral to a unilateral cut. Additionally, if the NE intermediate enzyme tyrosine hydroxylase was inhibited by alpha-methyl-para-tyrosine methyl ester, and the LC was electrically stimulated, causing depletion of NE, a similar decrease in GIF and SGV was seen in the hilus. Again, if the LC was stimulated on one side, the ipsilateral side decreased more. These results indicate that the varicosities and vesicles are NE containing and are correlated with one another due to their simultaneous decrease in number after LC activation followed by NE liberation. In addition, they reported that most likely, the NE terminals were synapsing mostly in the hilus, then the molecular layer, and finally least in the granule cell layer directly.

Crutcher and Davis (1980) compared the fields of α and β receptors to the amount of NE innervation in the hippocampus of adult rats. They used tritiated dihydroalprenolol (DHA) for β-receptor localization and tritiated WB-4101 for the α-receptors. For localization of NE and terminals, they used glyoxylic acid and a radioenzymatic technique utilizing phenyl ethanolamine-N-methyltransferase (PMNT). The largest amount of NE was found to be in the dentate hilus (infragranular region) with less in CA3 and even less in CA1. Biochemical measurements indicated the amount of NE in the DG to be 0.57 ± 0.07 μg/g and in the rest of the hippocampus

6

to be 0.30 ± 0.05 μg/g. Beta-adrenoceptor binding of DHA was similar between DG and Ammon's horn, whereas, σ-adrenoceptor binding was 30% higher in the DG than the rest of the hippocampus.   Oleskevich et al. (1989) using tritiated NE observed that the greatest number of NE-labelled varicosities were present in the molecular layer of the subiculum, the molecular layer of CA1, the polymorph layer of the DG, and a narrow zone in both CA3-a and CA3-b. The highest density of varicosities was found in the DG polymorph layer (2.5 million varicosities/mm^3).

In summary, the evidence presented above indicates a relatively dense NE innervation of the hippocampus and the densest input within that zone to the DG and the molecular layer of CA1 (lacunosum moleculare in figure #1). Beta receptors seem to be rather evenly distributed over the whole hippocampus and 70% of them are of the β1 subtype. Alpha receptors are 30% more numerous in the DG than the rest of the hippocampus and are mostly of the σ1 subtype. It is also evident that the largest field of NE synapses is present in the hilar region of the DG and more specifically in the subgranular region (zone 4 and just below the granule cell layer in figure #1).

NE and Dentate Units:

Few studies have been performed evaluating the effect of NE on DG cells. An

7

early series of studies to evaluate NE effects on units in the hippocampus was performed by Segal and Bloom (1974a & b-76a & b). The rats were anesthetized with halothane (0.5-3.5% fluothane). Acute cell recording was done using glass micropipettes filled with 3M NaCl. The tip diameters were $1 \mu m$ or less. In chronic animals, $62.5 \mu m$ insulated nichrome wire was used for recording. Bipolar stimulating electrodes ($200 \mu m$ twisted, insulated nichrome wire) were used for LC stimulation. Segal was the first to characterize NE action as that of increasing the signal-to-noise ratio for meaningful cell activation. In the first paper of the series, they found that putative pyramidal cells in layers CA1, CA2 and CA3 were inhibited by iontophoresed NE. Many of these cells had the characteristic bursting pattern, ie. complex spikes (a stair step burst characteristic of pyramidal cells (Fox and Ranck, (1981))). The inhibition appeared between 5-30 s. after the start of the drug ejection current (67.6 nA) and lasted for 10 s.-6 min. after termination of drug ejection. Similarly in the second paper, with electrical stimulation of the LC. When a train of pulses was used (10/s., 0.2 ms, 0.2 mA train) to stimulate the LC, inhibition lasted for 5-120 s. after cessation of the stimulus. Single pulses or short trains of high frequency stimulation (20 ms, 500/s.) failed to completely inhibit cell firing but a reduction of firing was present for 300-400 ms after the stimulus. The onset of the inhibition for

8

the high frequency trains (20 ms, 500/s.) was 150-200 ms. after the onset of LC stimulation.

In the third paper of the series, a portion of the sampled units was found in the granule cell layer (8/52 cells) and again inhibition was the primary effect of LC stimulation. Segal and Bloom trained rats to self stimulate (SS) with the stimulating electrode near the LC (0.25-1.5 sec. train of 30-50 Hz monophasic 0.2 ms pulses, 30-100 μA). They looked at the spontaneous activity of the recorded neurons and assessed changes after LC stimulation by the experimenter or through self stimulation by the animal (ie. presumably NE released from terminals in the dentate). Inhibition of spontaneous unit activity after LC stimulation was mainly found. The effect began 50-150 ms. after the end of stimulation and lasted for 300-800 ms. The degree of inhibition was different for the two different subject groups (SS group and single pulse group, ie. those animals who did not self stimulate). Cell inhibition in the self stimulating group was more pronounced than in the single pulse group (average decrease to 37% of baseline and 71% of baseline respectively). Cell firing rates seemed to be in a range of 6-20 Hz. Three out of eight of the recorded nonbursting cells were unaffected by the LC stimulation in the SS group even when bursting cells were inhibited in the same preparation. However, the point was made that there were

9

no differences in the inhibitory effects of NE on cells from both regions of the hippocampus (Ammon's horn and DG). Amphetamine (3-4mg/kg) given intraperitoneally (i.p.) mimicked NE actions, and tended to elevate SS rates and even cause non-SS rats to self stimulate. The cellular effects of this drug were harder to interpret because it lowered the baseline firing rate of the cells. However, Segal and Bloom found 3 cells where the inhibitory response was increased by the amphetamine. Diethyldithiocarbamate (DDC, 200 mg/kg) given subcutaneously blocks dopamine-β-hydroxylase, an intermediate enzyme in the production of NE. The inhibitory response of cells to the stimulation of LC was antagonized by this drug. The responses of cells were also significantly reduced by chlorpromazine. Finally, cell inhibition was also blocked by α-methyl tyrosine and 6-OHDA. SS behavior was also eliminated by these two substances which inhibit NE synthesis and deplete NE stores respectively.

In the fourth paper of the series, the cell types were not specifically explained and referred to only as bursting or non-bursting cells presumably from area CA1. First, they recorded cell firing changes as a result of an auditory stimulus (90 dB) administered for 2 s. every 30 s. Thirty-six out of 45 cells responded with inhibition of their baseline firing rate. All of the responding cells (36 of the 45) had a characteristic bursting pattern (presumably complex spiking), whereas 4/9 of the non-

10

responding cells did not burst. There was also a high correlation (0.85) between the magnitude of inhibition for the tone and the inhibition from LC stimulation on the ipsilateral side (delivered by a stimulating electrode placed near LC), indicating that the cells inhibited by LC stimulation would most likely be inhibited by the tone. DDC, chlorpromazine and 6-OHDA all blocked the inhibitory effect of the tone stimulus.

The next experiment paired the behaviorally reinforcing stimulus (LC stim. at levels high enough to support SS) with the behaviorally insignificant stimulus (tone) to ascertain whether the response would be augmented (ie. tone→ 1 s.→ LC stim.). The inhibitory responses to the tone were increased when paired with the LC stimulation. Again, non-bursting cells showed no change in either paradigm. When the tone was paired with food (sweet milk), a conditioned behavioral response (licking the milk) was seen, and a conditioned excitatory cellular response to the tone was observed in response following the pairing of tone and food. When LC stimulation was paired with the tone and food, the LC stimulation increased the new excitatory response in 13/15 animals. Additionally, in 2 cells with inhibitory responses, the LC stimulation potentiated this inhibitory response.

These initial studies indicated an inhibitory effect on the spontaneous activity of recorded cells in the hippocampus by LC stimulation (presumed release of NE from

11

terminals in the hippocampus). The conditioning study suggested something even more interesting, the effect of LC stimulation is to enhance a cell's response whether excitatory or inhibitory. This led to the proposal by Segal and Bloom that NE did not produce a simple transmitter effect, but increased the signal-to-noise ratio of cell responses to significant stimuli.

Pang and Rose (1987) were the next group to assess NE effects on DG units. They evaluated the effects of directly applied NE on characterized θ-interneurons recorded from just below the granular cell layer.   Hippocampal interneurons have been referred to as theta cells because they are known to be strongly modulated by the theta rhythm in the EEG of the hippocampus (Jung and McNaughton, 1993). The rats were anesthetized with either urethane (1.5g/kg) or sodium pentobarbital (50mg/kg). Monopolar stimulating electrodes were used to activate commissural afferents and entorhinal cortex afferents. Recording electrodes were multi-barrel glass micropipettes containing 5M NaCl and in some cases 50 mM glutamate to enhance spontaneous recording. Filters were set at 500 Hz-10000 Hz for unit recording and unfiltered action potentials were measured at 0.5 Hz-10000 Hz. They recorded from 203 hippocampal neurons and found that NE excited 79/94 θ-interneurons (~mean baseline rate pre NE: 10 Hz. Mean rate post NE: 30 Hz). Interneurons were

characterized by their firing pattern through the EP trace. They fired in single spikes all along the length of the trace. They observed that the effects of NE on θ-interneurons from DG and CA1 were not significantly different from one another which suggests a similar mechanism for both effects.

With antagonist application, Pang and Rose found that for the θ-interneurons, the α2-antagonist rauwolscine and the β-antagonist timolol significantly blocked the excitatory effect of NE on these neurons. Prazosin, an α1 blocker, had no effect.

Pang and Rose (1989) extended the study of the effects of NE on dentate cell types to include granule cells. Using urethane anesthetized rats (1.5 g/kg), they characterized granule cells electrophysiologically by their unfiltered action potential duration ($\leq$ 0.4ms), predominance in the granule cell layer (designated as 150 μm below the negative-positive reversal site for the PP-EP), activation at short latency by a PP pulse ($<$ 5ms), and finally their firing characteristics which were mainly single spikes even at high stimulation intensities.

Again, the interneurons were characterized by their firing patterns. They found that pressure ejected NE (5 x 10^{-3}M) depressed the spontaneous firing of 18/21 granule cells recorded (mean firing rate before NE approx. 15 Hz and after, approx. 3

13

Hz). One granule cell was excited and two others gave biphasic responses. They found that isoproterenol (ISO, 10^{-4}M) applied similarly, excited 4/4 granule cells. Similar to the 1987 study, they found that NE excited 19/24 interneurons (mean rate before NE approx. 7.5 Hz and after, approx. 16.5 Hz), 3 were inhibited and 2 had biphasic responses. Isoproterenol also excited 5/5 of the interneurons. The inhibitory effects of NE were said to be mediated by the α1-receptor and the α2 and β-receptors mediated the excitatory effects. The results of this study indicate that interneurons and granule cells are affected similarly (excitation) by the β-receptor agonist isoproterenol. NE, however, causes depression of firing in granule cells and excitation in interneurons.

NE and Intracellular Recording in Vitro:

Lacaille and Schwartzkroin (1988) recording intracellularly from the in vitro dentate slice assessed the effects of iontophoresed NE on granule cell excitability. In 12/16 of the granule cells responsive to NE, there was a depolarization of the membrane. The mean membrane potential was -62 mV. The depolarization had an amplitude of 10.4 $\pm$1.7 mV, reached a peak in 1.4 $\pm$0.9 s. and lasted for 17.2 $\pm$4.5 s. The depolarization caused by NE was obtained at near resting membrane

14

potential and was described in terms of the closing of K⁺ channels.

Gray and Johnston (1987) using the in vitro slice preparation assessed the effects of NE on granule cell activity in whole cell or patch clamp experiments. The bath and pipette solutions were formulated to block all potassium (K^+) and sodium (Na^+) currents with tetrodotoxin (TTX) and 3,4-diaminopyridine (3,4-DAP). Pressure ejection was used to deliver drugs in single or double-barrelled pipettes, near the soma of the clamped cell. In the whole cell clamp experiments, the step depolarizations were initialized from a starting potential of -60 mV up to -35 mV. This depolarization activated a Ca^{2+} mediated inward current which increased in intensity as the command potential became more depolarized. The protocol for testing NE effects began with holding the cell at a clamped voltage of -60 mV and stepping it to 0mV every 7-15 s. Once a stable baseline was acquired, a pulse of NE was applied to the cell. An increase in the amplitude of the Ca^{2+} mediated inward current occurred approximately 20 s. after the NE was applied. The β-receptor agonist isoprenaline similarly increased the inward current (37 ± 11%).

Clonidine, an α2-receptor agonist did not alter the inward current. NE also increased the amplitude and duration of Ca^{2+} action potentials. The cyclic AMP activator forskolin increased the inward current (18 ±3%) as did 8-bromo-cAMP (44

15

±20%). Single channel patch clamp recordings done with stepwise voltage changes from -100 mV to -10 mV showed an increase in probability of the same Ca^{2+} channel opening in the presence of isoprenaline. Patch clamps done with different command voltages showed increased open times for the Ca^{2+} channels mediating the inward current. The same held true for NE application and 8-bromo-cAMP application.

Madison and Nicoll (1986) studied NE effects on intracellularly recorded rat hippocampal CA1 pyramidal cells in the in vitro slice preparation. They found that there was a slight depolarization of the membrane after NE application and this was mediated by the β-receptor as was determined from the similar effect produced by β-receptor agonist isoproterenol. The slight depolarization was paired with a finding that the afterhyperpolarizations of the cell were decreased. In a second paper, Madison and Nicoll (1986) demonstrated by the use of cAMP analogues that the effect could be mimicked by activating cAMP indicating its importance in these NE effects.

These three studies all found that the effect of NE on different cell types in the hippocampus is depolarization.

Discrepancies in Single Unit recording:

Results of the single cell work present a problem for a simple characterization

16

of NE effects on cellular activity. Segal and Bloom found that all NE-affected cells were inhibited in all subfields, while Pang and Rose found interneurons to be excited by, and granule cells to be inhibited by direct NE application, but β-receptor activation alone excited both types. The in vitro intracellular studies all produced similar results which included increased depolarization of the principal cells (granule and pyramidal cells). This finding is consistent with NE induced excitation. These results indicate marked differences in findings between labs using similar paradigms.

Caveats for Unit Recording Studies:

Self-Stimulation: Caveat 1:

There is an inherent problem in using self stimulation of LC as a criterion for effective activation of the NE system. Mainly, there is evidence that this paradigm is not dependent on the NE system. NE depletion does not typically reduce or inhibit self-stimulation in the vicinity of LC, nor does dorsal noradrenergic bundle lesioning affect LC self-stimulation (Corbett et al., 1977; Corbett and Wise, 1979). In addition, Harley et al., (1989) found that the β-receptor antagonist propranolol did not block the effects of electrical LC stimulation in the hippocampus, while the effects of LC

cell activation were prevented.

Armstrong-James and Fox (1983) observed the effect of iontophoresed NE on superficial (0-800 μm) and deep (800-1400 μm) neurons in the somatosensory cortex. These neurons could be differentiated via their spike amplitude, firing rate, and firing pattern. They also used a voltameter (device for measuring the catecholamine oxidation potential) to measure the actual level of iontophoresed NE coming out. Deep cells had higher firing rates and larger spike amplitudes. The deep cells exhibited many more spikes per burst than did the superficial cells. With two distinct groups of cells maintained, they observed the effects of low concentrations (5×10^{-8}-5×10^{-7}M) and high concentrations (up to 100x the previously mentioned doses) of NE on these cells. Superficial cells were inhibited with low NE current and stopped firing completely following larger currents. Deep cells were often excited at low current and inhibited at larger currents. A few cells in the deep zone exhibited a long-lasting increase in firing rate after NE application. These effects lasted up to an hour after application of NE and only occurred at the low current range for NE which was lower than had been employed in other iontophoretic NE studies. The authors suggest that the physiological

18

effects of NE are better reflected by the lowest effect currents and that the common description of NE as inhibitory may be due to the use of unphysiologically high NE levels. While this accounts for many inhibitory NE reports, and may explain the iontophoretic effects of Segal and Bloom, it would not account for the inhibition findings of Segal et al using presumed physiological release of NE via self-stimulation.

Cell Identification: Caveat 3:

Amaral (1978) described cell types in the hilar region of the DG in rat using the Golgi staining method. Four zones were used to demarcate the various layers and areas in the hilus (see fig. 1). Zone 1 was simply the continuation of the pyramidal cell layer into the first portion of the hilus. Here there were pyramidal cells, pyramidal basket cells, pyramid-like stellate cells, and giant aspiny stellate cells (most likely an interneuron). Zone 2 contains the inferior region unipolar (IRU) interneuron (Amaral and Woodward (1977)). Its axons collateralize mainly within the dendrites of the pyramidal cell layer but branches are sent to stratum oriens and radiatum. Similar cells to this type have been seen in the deep hilus (dorsal zone 4 in figure #1) with dendrites projecting into the fascia dentata. Large spiny stellate cells and pauci-spined cells (small spherical somata with only a few spines on the dendrites) are seen in both the

19

stratum radiatum and zone 4 (hilus). According to Amaral, these cells have no thorny excrescences on their dendrites and they all have axons characteristic of interneurons. Furthermore, their alignment perpendicular to the incoming fibres indicates they are specialized to function at the interface of the fascia dentata and the rest of the hippocampus. Some of the neurons in zone 3 have dendrites which only project towards the granular layer. These may be unaligned pyramidal cells.

One particular cell type seems to be quite prevalent throughout zones 2,3,and 4. It is the aspiny suprapyramidal stellate cell. Their axons perforate the granule cell layer and enter the molecular layer of the dentate. These axons run parallel to the pyramidal layer. In zone 4, most of the neurons were aspiny and found on the border between the granule cell layer and the hilus. The first is the dentate basket cell (2 types). The apical dendrite travels up through the granule cell layer and branches out into the molecular layer where many axo-dendritic connections were seen. The basal dendrites penetrate into the hilus and some complex with mossy fibre terminals. The axon arises from the apical dendrite and also runs through the molecular layer. The second type of basket cell sends dendrites along the top of the molecular layer and these make contact deep in the hilus. The axon tends to originate from the cell body rather than the apical dendrite as compared to the first type of basket cell. The

spheroid cell also borders on the granule cell layer. Its spineless dendrites flow into the dentate and the hilus. Its axon contacts the granule cell layer and the molecular layer. Another type of aspiny neuron sends bifurcations of its axon to both the dentate and hilar regions. The mossy cells are found mainly in zone 4 and their dendrites have spines. The dendrites are long and narrow and seem to cover large areas of the hilus. These dendrites do not often penetrate the granular layer and are seldom seen in continuity with the pyramidal layer. The axon breaks up into many branches, some of which go to the molecular layer of the dentate and the rest project out of zone 4 into the fimbria. Three more cell types have been seen in zone 4. They are the aspiny stellate cell, the long-spined multipolar cell and the oviform cell. In all, 21 cell types have been described by Amaral in the hilus of the hippocampus. Many of these have characteristics which may be interpreted as being interneuron-like. The electrophysiological characteristics of all these cells have not been described. Therefore, many interneuron-like cells may have markedly different electrophysiology. If sampling bias effects occur due to extracellular recording or anesthetic characteristics, then Pang and Rose (recording near the granule cell layer) and Segal (less clear about areas of recording) may be looking at different cell subpopulations.

The Evoked Potential:

In the DG, the PP terminals synapse on the dendrites of the granule cells about 100 μm from the soma and make an excitatory connection (Andersen and Loyning, 1962; Fujita, 1962). Inhibitory interneurons synapse on or nearer to the somata of the neurons (Blackstad, 1958; Andersen, 1966) (The description from Amaral above indicates this is an oversimplification). Andersen et al. (1971) recorded evoked field potentials from the DG which were orthodromic (ie. following the fibre tract connections in the same direction), stimulating perforant path and recording from granule cells. They also recorded antidromic field potentials (stimulating fibre tracts opposite to their direction of flow) by stimulating MF and recording in granule cells. In the subsequent unit analysis of the evoked potential (EP), they found that unit action potentials corresponded with the negative wave of the population EP which was called the popspike, while the positive wave was indicative of an EPSP component. When stimulating the perforant path, the subsequent unit discharges in the granule cell layer corresponded to the popspike portion of the EP and were assumed to be granule cells activated by the stimulus (see figure 2).

22

Neuman and Harley (1983) first observed a long-lasting potentiation of the population spike of the DG following NE iontophoresis at the granule cell layer. This is only the second example of a long term functional plasticity in the DG. NE seemed to increase the potency of the glutamatergic perforant path response. The increase in the amplitude of the population spike did not occur immediately with iontophoresis of NE, but happened between 30 seconds and 8 minutes after initiation of iontophoresis. Sixteen out of 41 experiments resulted in long term enhancement of the popspike amplitude (lasting longer than 30 minutes) and the mean maximum potentiation, 130-140% of baseline, was seen after 30 min. The rest of the sites yielded short term enhancement lasting under 30 minutes with maximum potentiation of the popspike ranging from 20-400% of control values. Generally, there was no consistent EPSP amplitude change. A similar potentiation effect on popspike amplitude, but not the EPSP had been reported previously with electrical stimulation of LC (Assaf and Miller, 1979). This potentiation, however, was maximal 40 ms. after the onset of LC stimulation.

Goodchild et al (1982) first employed the method of naturally activating cell

23

bodies with the native transmitter, glutamate, to cause synaptic release from terminals in the brain. This preferentially activates cell bodies, which are responsive to the neuroexcitant, rather than fibres of passage. Harley and Milway (1986), using 100-150 nL pulses of glutamate in or near the LC, found long-lasting PP-popspike enhancements in 40% of the animals tested and short-lasting effects in all experiments. The population spike average maximal increases were 141% above baseline, with mean onset of a significant 30 sec. average increase 1.1 min. after glutamate ejection and largest change occurring at 1.6 min. after ejection. In 18/20 animals, the population spike returned to baseline levels by the end of the experiment. The average time to the return to baseline was 8.4 min. However, 5/19 monitored for 20 minutes or longer after glutamate ejection showed effects lasting > 20 min. The population EPSP slope also changed in 13/20 animals. The increase began 0.8 minutes after glutamate ejection and reached a maximum of 112% at 1.2 minutes after ejection. It returned to baseline by 3.2 minutes after ejection. These effects were blocked by propranolol (30 mg/kg i.p.).

Harley et al. (1989) reported a difference in the potentiation achieved by LC electrical stimulation and LC glutamate stimulation. Glutamate stimulation of the LC caused a potentiation of the PP evoked population spike which could be short-lasting

(< 30 mins. with return to baseline) or long-lasting (> 30 mins.). Brief electrical stimulation of the LC reliably caused an immediate, short-lasting potentiation of the population spike, but repeated pairings of the electrical LC stimulation and the PP evoked population spike resulted in long-lasting potentiation in 10 out of 22 experiments. However, the β-receptor antagonist propranolol did not block the electrical LC stimulation effect, but did block the glutamate LC stimulation effect. This indicates that there may be two separate systems mediating these potentiation effects, and only selective chemical activation of LC provides potentiation dependant on the β-receptor in DG (Harley and Evans, 1988). It is now accepted, based on work both in vivo and in vitro, that the effect of NE on the PP-EP in the hippocampus is an increase in population spike amplitude which may be long-lasting or short-lasting and which is mediated through a $\beta 1$-receptor, cAMP dependent system. More recent research in whole animal has indicated that glutamate activates LC cells immediately but the PP-EP increase is not seen immediately (Harley and Sara, 1992)

In Vitro Preparation:

Data obtained from the hippocampal slice preparation suggested the duration of application of NE may determine whether there will be short-lasting or long-lasting

25

potentiation. Lacaille and Harley (1985) using a 10 minute bath application of NE (at a threshold concentration of 10 μM) produced long-lasting potentiation in only 25% of the slices. Fifty-three percent of the slices exhibited an EPSP slope increase to a mean of 117% of control. Seventy-six percent of the slices exhibited significant increases in population spike amplitude with a mean of 131% of control. Stanton and Sarvey (1985b) using a 30 minute bath application of NE (50 μM) produced a long-lasting potentiation in all experiments. These long term effects could be followed for up to five hours after NE wash-out. Another important finding from Stanton and Sarvey was that long-lasting potentiation was blocked by the protein synthesis inhibitor emetine and the addition of forskolin (an adenylate cyclase stimulant) enhanced the response. Finally, both Lacaille and Harley, and Stanton and Sarvey provided evidence that the in vitro potentiation was β-receptor mediated. It could be blocked by the β-receptor antagonist propranolol (Lacaille and Harley) and by the specific β1-receptor antagonist metoprolol (Stanton and Sarvey).

Stanton and Sarvey (1985a), also using the slice preparation, showed that if NE was depleted using 6-OHDA, high frequency induced LTP was eliminated. Similarly, the β1-receptor blocker metoprolol eliminated both high frequency induced LTP and NE induced long-lasting potentiation. Burgard et al., (1989) observed that NMDA receptor

antagonists also blocked both NE-LLP and LTP in the DG. Still using the slice preparation, they applied APV or CPP to the bath and found that both LTP and NE potentiation were blocked as evidenced by the lack of increase in population spike amplitude. They also added that the antagonists alone did not alter the population spike. Again using the hippocampal slice, Chetkovich et al (1991) showed that activation of the NMDA receptor by glutamate increases the levels of cAMP in layer CA1. This could be blocked by APV and by the removal of extracellular Ca^{2+}. In the whole animal, however, NE depletion does not prevent LTP and newer data suggest NMDA currents may not be necessary for NE induced potentiation (Frizzell ands Harley, 1994).

Although the intracellular mechanism of the NE effects is unclear, the reliability of the potentiation effect with NE or LC activation is not. In vivo effects with chemical activation of LC are also consistently blocked by β-receptor antagonists systemically (Harley and Milway, 1986) or locally in DG (Harley and Evans, 1988). Glutamate activation of LC would appear to be an excellent method of inducing synaptic NE release. Additionally, the enduring functional change in the DG produced by LC-NE in the PP-EP is of intrinsic interest as a model of PP-DG synaptic plasticity.

There are 3 main hypotheses describing hypothetical NE effects which might explain NE potentiation of the PP-EP.

Signal-to-Noise hypothesis:

Segal and Bloom (1976b) initially hypothesized that the role of NE was to increase the signal-to-noise ratio for evoked activity in the hippocampus, enhancing whatever cell response, excitatory or inhibitory was evoked by the stimulus. Similar results have been seen in sensory systems where NE inhibits spontaneous cell firing and allows sensory activation to produce a larger, or cleaner response relative to background (Woodward et al., 1979). Similar results have been described in the cerebellum. Freedman et al. (1977) found that the effect of NE iontophoresis onto the Purkinje cells in the cerebellum was to inhibit spontaneous activity, while affecting the evoked activity of mossy and climbing fiber stimulation less. This supports the hypothesis of NE increasing the signal-to-noise ratio. The reduction of spiking during the excitation caused by a mossy fiber input was less than the reduction of background activity during NE iontophoresis. The net result here was an improvement of the signal to noise ratio of the synaptically evoked event over the background

spontaneous firing rate. Woodward et al. (1979) addressed the issue of whether these NE effects on Purkinje cells were pre- or post-synaptically mediated. They assessed the effect of iontophoresed NE in conjunction with other neurotransmitters. They found that NE increased the effectiveness of GABA induced inhibition of Purkinje cells, but, they found that NE also increased the effectiveness of glutamate induced excitation of Purkinje cells. This effect was also seen with electrical stimulation of the LC (3.5 s. at 10 Hz). They concluded that NE enhanced the effectiveness of GABA and glutamate which facilitated information transfer in the cerebellum. An increase in response to glutamate input with increased GABA sensitivity could account for Purkinje cell enhancement and may also account for a larger population spike in DG. Increased glutamate and GABA sensitivity may produce a larger EP.

Disinhibition Hypothesis:

A second view of NE's action is the disinhibition hypothesis. Gyorgy Buzsaki (1984) proposed that neuromodulators like NE act to decrease inhibitory interneuron activity thus allowing the principal cells to become more depolarized. This disinhibition requires that inhibitory interneurons themselves be inhibited. Milner and Bacon, (1989) using light and electron microscopy with immunoautoradiography observed that there is

overlap between the distribution of GABA and catecholaminergic terminals in the DG. Excitatory and inhibitory terminals synapse on common targets, and GABA and catecholamine terminals occur in apposition to one another. So, catecholamine terminals are well placed to modulate inhibition. Hendricks and Teyler, (1983) blocked GABA-mediated inhibition with bicuculline or picrotoxin and found that induction of long-lasting synaptic potentiation in the hippocampus is facilitated as well as a large increase in the maximal potentiation that could be induced. Suzuki and Smith (1983) observed that blockade of GABA-meditated inhibition by bicuculline increased the amplitude of sharp waves (apical dendritic depolarizations of pyramidal cells. Buzsaki et al., 1983) and the number of pyramidal cells firing synchronously in hippocampus. In summary, reduction of inhibitory interneurons as shown in Segal and Bloom (1974) and the other studies above by Buzsaki et al. and Hendricks et al., would lead to increased response of granule cells to their PP, glutamatergic input. Neither of these hypotheses however, would readily account for the long-term increase in responsiveness which is often seen.

NE-Long-Lasting Potentiation Hypothesis:

This hypothesis would suggest that the larger response to input in the system

is caused by a change in the synaptic efficacy which might be mediated in either or both of two possible ways, presynaptically or postsynaptically.

Presynaptic Plasticity:

The circuitry change mediated presynaptically would be caused by a long term increase in the amount of neurotransmitter released from the synapse. This may happen, for example, with a physical increase in the number of synaptic vesicles released or by a decrease in activity of reuptake mechanisms. This type of plasticity would cause an EPSP increase for the length of time the plasticity lasted. Increase in glutamate transmitter release following NE pre-exposure has been reported in DG (Lynch and Bliss, 1986) and an increase in phosphorylation of synapsin proteins I and II following isoproterenol exposure and an increase in synaptic transmission in DG (Parfitt et al., 1992) has also been reported. Both effects depend on β-receptor activation as seen for NE-EP potentiation. Consistent with an enduring change in synaptic efficacy is the evidence of 2nd messenger and NMDA receptor involvement in NE potentiation.

Postsynaptic Plasticity:

A postsynaptically mediated plasticity would generally increase the likelihood of

an action potential from a normal stimulus. This would involve an increase in synapse-to-cell coupling. This might reflect a general increase in excitability or could be a more selective facilitating current spread from a localized site. Changes in threshold do not appear to accompany EP potentiation as antidromic EP's are not altered (Lacaille and Harley, 1985). However, cells appear to fire more to PP-input than can be accounted for by EPSP changes alone. A similar long-term enhanced synaptic coupling has been seen with frequency induced long-term potentiation. This synaptic enhancement might be selective to particular spines on the dendrite for example. The enhanced coupling of those spines to action potentials would result in a stronge response.

Hippocampal Theta Rhythm:

The hippocampus has an EEG potential which oscillates with a certain frequency when an animal engages in or ceases certain activities. This oscillatory synchrony is thought to be important because it can bring differing brain structures into a resonance state and aid in effective information processing. Green and Rawlins (1979) reported the first evidence of hippocampal generators of theta (defined as rhythmic oscillations) gathered by Green et al. (1960) and later Bland et al. (1975 &1976). These generators were found to be in the CA1 region of the hippocampus

proper and the stratum moleculare in the DG. The generators are the areas where theta is induced and maintained.

There are three basic categories of EEG rhythmicity in the DG. The first is type 1 theta, which occurs during voluntary movements such as walking or running. It has a frequency range of 6-12 Hz and is resistant to atropine. The next type is referred to as type 2 theta, and occurs during alert immobility in response to sensory stimuli. It has a frequency range of 4-9 Hz and is sensitive to atropine. The final rhythm is referred to as LIA (large irregular amplitude) and is present during chewing, grooming and alert immobility.

Hippocampal Cells and Theta:

The theta rhythm itself is reflected in the membrane oscillations of groups of cells. The actual group of cells involved in the maintenance of theta is controversial. Fox and Ranck (1981) were among the first to provide evidence that local circuit inhibitory interneurons were theta cells, meaning their activity increased with theta onset and they were phase locked with the theta rhythm. This view is one of the most widely accepted. However, Bland et al. (1980) presented evidence that CA1 pyramidal cells and dentate granule cells were also theta cell types, ie. indicating that

theta interneurons were not necessarily the only source of the theta rhythm. Rose et al. (1983) also stated that dentate granule cells were theta cells. Buzsaki et al. (1983) proposed that his physiologically identified interneurons and granule cells were theta cells. More recent research however, suggests that granule cells, like the principal cells of CA1 and CA3, are not high firing cells with a rate like the theta rhythm, but have low firing rates which decrease during theta, although rate modulation may occur. It is the interneurons which seem to be the theta cells.

While most earlier authors described granule cells as increasing activity with induction of theta and firing with high rates in a rhythmic fashion, more recent studies including intracellular studies indicate that this is not the case. Jung and McNaughton, (1993), using chronically implanted electrodes in freely moving rats, classified cells on the basis of their electrophysiological characteristics such as firing suppression as a result of paired-pulse stimulation, firing rate, spike width, spike height and histology. They found granule cells to be low rate (0.1⅝ Hz), occasionally bursting cells which fired only once in the popspike window, were inhibited in low inter-stimulus-interval paired pulse tests and were not modulated to the theta rhythm. Interneurons were found to be high rate cells which did not burst, fired multiply along the popspike trace and were modulated closely by the theta rhythm. Scharfman,

(1992) using the slice preparation, recorded intracellularly from both granule cells and interneurons. She found that granule cells have very low spontaneous activity and have moderately wide action potentials. Oppositely, she found that interneurons have narrow action potentials and high rates of firing compared to granule cells.

Theta Cell Types:

Bland et al. (1989) have recently identified two different main types of theta cells. The first type are the theta-on cells, both phasic and tonic. The phasic cells are the classical theta cells that increase their firing rate and fire rhythmically in concordance with the theta rhythm when it is present. The second type are the theta-off cells, which also have phasic and tonic subtypes. These cells reduce their firing rate when the theta rhythm is induced. This new physiological data is consistent with the anatomical evidence for a multiplicity of interneuron types.

Transmitters and Theta:

A series of studies of EEG activation have indicated that the cholinergic, and more recently, serotonergic systems solely control this rhythmic activity in the brain (Vanderwolf, 1988 & Vanderwolf et al., 1993). NE was, until quite recently, not thought to be involved in the control of EEG. Early studies provided no evidence for an

NE role in theta generation. Robinson et al. (1977) found three important results which suggest that NE (via LC) is not involved. After NE depletion with 6-OHDA, type 1 and type 2 theta (hippocampus) and low voltage fast activity ((LVFA) neocortex) were intact and occurred normally. Secondly, when brain dopamine and NE were depleted by injections of α-methyl-p-tyrosine, activity as above remained stable. Third, electrical stimulation of the LC was "relatively ineffective" in producing behavioral changes or type 1 and 2 theta in the hippocampus and LVFA in the cortex.

A New View:

Recently, using chemical LC stimulation new evidence suggests NE does play a role in theta induction. Berridge and Foote (1991) directly activated the LC with the cholinergic agonist bethanecol (70-135 nl, 1 ng/nl, 5 mM) given over a 60 second period and recorded EEG in the cortex and dorsal hippocampus. They observed an increase in fast wave activity in the cortex and a switch to theta in the hippocampus beginning between 5 and 30 seconds after the onset of LC activation. The recovery was two-stage with the first stage being recovery of low power frequencies within 2-5 min. The second stage involved recovery of higher power frequencies within 10-15 minutes. Placement in the LC was verified by the increase in LC neuron firing (3-5

36

times the baseline rate) which occurred with injection placements as much as 200-500 μm medial or lateral to the LC. This is similar to the anatomical range found with glutamate ejection for EP potentiation. The theta activation effect was blocked by propranolol (200 $\mu g/4$ μl i.c.v.), like the EP potentiation effect, and by clonidine (α-receptor antagonist 50 $\mu g/kg$ i.v.). This indicates that NE release is important in the mediation of this effect. They suggested that the block caused by clonidine may have been caused indirectly by its anesthetic properties. However, the block caused by propranolol cannot be attributed to anesthetic properties. If NE induced theta reliably, this might contribute to long-lasting potentiation of the PP-population spike since theta gated input can promote potentiation at DG synapses. At the cellular level, theta induction would be expected to correlate with increased firing of some interneuron populations.

Present Work:

The primary focus of the present study is to investigate the effects of synaptically released NE on the activity of single cells in the DG in vivo.

Glutamate ejection in the vicinity of the LC will ₃ employed to activate NE release and the PP-EP will be monitored to assist in locating the recording electrodes

in the DG and to record the occurrence of population spike facilitation as a marker of successful NE release in DG.

Concomitant recording of unit and EP changes in the DG will shed light on the relationship between changes in spontaneous unit activity and changes in the EP due to NE release, and provide one test of the disinhibition hypothesis.

Dentate gyrus EEG will be monitored to evaluate the recent hypothesis that NE release triggers the theta rhythm and again the temporal relation among unit, EEG and EP change will be a focus of interest. These experiments should shed light on the ways in which physiological NE release affects the DG circuit and promotes functional plasticity.

METHODS

<u>Subjects:</u>

Fourteen Sprague-Dawley female rats, (Charles River Canada Inc., Montreal, Canada), weighing between 200 - 390 g provided data in this study. Anesthesia was induced in each subject with urethane (1.5 g/kg i.p.), supplements at 1/4 of the original dose were given as needed. After anesthesia each subject was stereotaxically placed with skull horizontal. A circulating hot water blanket, replaced later by an FHC temperature control unit with electric blanket, was used to maintain rectal temperature at 37.0° C - 38.5°C.

<u>Recording in Dentate Gyrus:</u>

A concentric bipolar stimulating electrode (Kopf NEX-100X) was placed in the PP (7.2 mm posterior, 4.1 mm lateral, 2.5-3.5 mm ventral relative to bregma) and 2 glass pipettes were placed in the DG (3.5 mm posterior, 2.0 mm lateral relative to bregma). The recording pipettes were mounted in a Narishige holder which holds one pipette stationary while allowing the other to be moved approximately 1 mm. in three directions relative to the stationary pipette. The two pipettes were positioned as close

together as possible (200-500 μm) to facilitate maximum similarity between the two PP-EPs (see figure #3). Depths were a function of EP similarity and ranged from 2.4-3.6 mm below brain surface. Both pipettes were heat pulled over a small carbon fibre (7 μm diameter) to a total diameter of ~10 μm and then filled with 3 M NaCl. The impedances ranged from 2-6 MΩ. Current (10 μA for 2 minutes) was passed through the unit recording carbon filled pipette for lesioning at the conclusion of each experiment. In some experiments, open-tipped single barrelled pipettes filled with 2% pontamine sky blue in 0.5 M sodium acetate were utilized in recording and dye marking of the DG site.

Glutamate Application and Recording in Locus Coeruleus:

A double-barrelled glass pipette was placed in or near the LC on a 20° angle posterior to vertical at 5.2 mm posterior and 1.2 mm lateral to lambda. One barrel was filled with 2% pontamine sky blue in 0.5 M sodium acetate. This barrel was used to record spontaneous single unit activity to aid in localizing LC (see figure #3). Lesioning was attempted by iontophoresing the dye from this barrel, but it was unreliable. The other barrel was filled with 0.5 M l-glutamic acid in dH_2O (ph=7.4). A tube was connected to the glutamate barrel from a Neuro-Phore BH-2 pressure
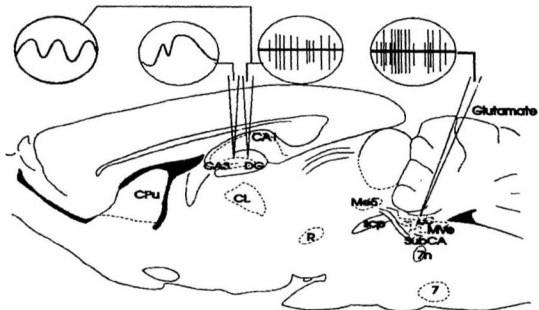
Figure #3: Saggital section showing the pipettes used for evoked potential recording in the dentate and the LC recording pipette (20° from vertical) and the associated glutamate ejection barrel.

ejection system. A 30 psi pulse was delivered through the tube to the pipette barrel ejecting a drop of glutamate. The drop volume was measured under a microscope. Manipulation of ejection time controlled the size of the drop and its size measured approximately 140 nl. Goodchild (1982) provided evidence that the actual volume in the brain tissue is about 68% of that estimated from the drop diameter in air. The tip size of each barrel was kept at 18 - 22.5 μm and the impedance ranged from 4-6 MΩ. On the top of the pipette, the recording barrel was cut shorter to allow the tube to be put on over the glutamate containing barrel.

In recording the spontaneous unit activity through the double-barrelled LC pipette, (differentially amplified at a gain of 10000-20000 and band passed at 600 Hz - 3 kHz → oscilloscope → audio unit) a depth profile could be made through cerebellum and dorsal pons as an aid in localization of LC units. This unit activity was not stored. When the pipette approached the LC, a series of tail and paw pinches were employed, as LC is known to respond with a burst of activity to this stimulus. The response is characterized as a short burst of activity (1.2 Hz up to 10 Hz for 100-500 ms) followed by a pause (Cedarbaum and Aghajanian, 1976). Testing also included opening and closing the jaw of the subject. The mesencephalic trigeminal nucleus borders the LC both laterally and anteriorly. There, cells respond to manual

manipulation of the jaw and aid in localization of the LC (Harley and Milway, 1986). The LC was typically encountered at 6.0 - 6.2 mm below brain surface. In addition to testing for cell characterization, the viability of the glutamate ejection was tested on cell layers in the cerebellum. Glutamate was ejected here to ensure the pipette tip was not blocked, as blockage did occur from time to time. In such a case, the tip was cut back to ensure glutamate was coming out and tip diameter, as well as drop volume was measured again. Dye injections were employed in marking LC recording sites. Glutamate was drawn out of the ejection barrel with a syringe at the end of the experiment while the pipette was in place and was replaced with 2% pontamine sky blue, which was then pressure ejected into the brain.

Recording:

Three different types of information were obtained from the two recording pipettes and received by three different Grass unity gain headstages. One pipette was used for one EP, while the other pipette via a Y-connector, yielded EP and EEG data to the other 2 headstages respectively. Differential recording of the EP was used to reduce the field potential artifact on the unit trace which was obtained from amplifying the resultant signal from the two pipettes.

This was not wholly successful with a large EP. It did prove useful for assessing unit activity during an EP subthreshold for a population spike. One EP was sent from the Grass differential amplifier (filters 1 Hz - 3 kHz, gain 100x) to an oscilloscope then to a Parc EG&G (signal subtraction) preamplifier (this was the unit signal that had the EP taken out). The other EP was sent to the computer for storage of the unaltered waveform (this was the EP used for data analysis). This same signal via a T-junction connector, was also sent to a Phonic 15 band, 2 channel graphic equalizer, to the oscilloscope and then on to the PARC subtraction preamplifier. The equalizer was used to make the two EPs as comparable as possible. Finally, these two similar signals were subtracted and the resulting signal was amplified via the preamplifier to become the unit trace (filters 300 Hz - 3 kHz, gain 200x). The EEG signal was fed directly into the computer for analysis (see figure #4).

Data Acquisition:

All signals were digitized and stored on a PC compatible 486sx/25 computer using the Datawave Technologies "Brainwave" software package. The LC electrode was first lowered appropriately and the LC was located electrophysiologically. Next, the two DG pipettes were lowered and cell layer population spikes were found. A unit

44
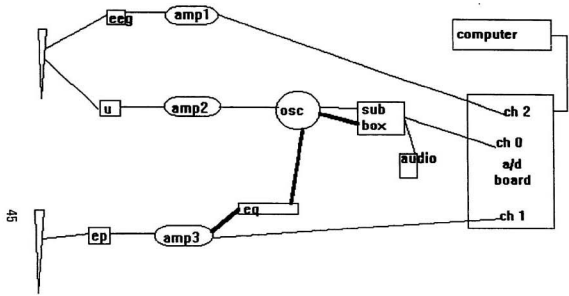
Figure #4: Schematic diagram of differential recording setup. Units (u) and EEG are taken from one dentate pipette, while evoked potential is taken from a second dentate pipette. The evoked potential signal is split and one goes directly to the computer while the other is used to subtract the "evoked potential" signal from the unit channel.

was then found in the region of the popspike and the EEG was recorded. A baseline for all three parameters was collected for 5 min. Glutamate was ejected into the LC after a minimum of 30 popspikes, after which, recording continued for 20 min.

Prior to data collection, cells were evaluated on the oscilloscope for their response to the sub and suprathreshold PP stimuli. Only subthreshold responses could be confidently determined. Following these observations, all 3 electrophysiological responses, EP, units, and EEG were monitored.

Evoked Potential:

To obtain the EP, a 0.2 ms monophasic, square wave pulse, 25 - 30 V, was delivered to the PP at 0.1 Hz. The EP was amplified 100x, filtered at 0.3 Hz - 3000 Hz and collected at a sampling frequency of 10000 Hz. Measurements taken in offline analyses were: amplitude of the population spike, slope of EPSP and height of EPSP (see figure #2). Latency measures were not taken, although average waveforms for the 5 min. periods before and after LC activation are shown in the results section. For final analysis, basic X-Y plots were done of the population spike amplitude and the EPSP slope and height using Quattro-pro. The spike amplitude and EPSP slope are reported as the maximal change relative to the average baseline. Confidence intervals

positive wave is
pop. EPSP.
(synaptic
component).

Negative
wave is
popspike
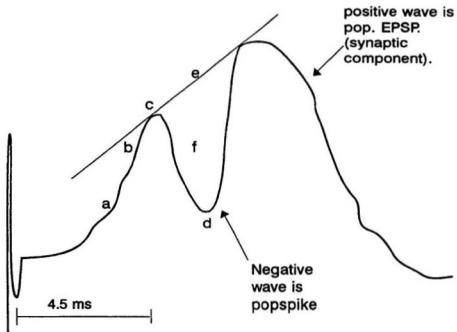
4.5 ms

Figure #2: Medial PP evoked potential starts ~4.5ms after stimulus.
Parameters measured are area under the tangent (f), and slope of
EPSP (b-a/change in time). The popspike (indicated) is the summed
depolarization of a group of granule cells.

were drawn for comparison of 5 min. averaged popspikes before and after the glutamate ejection.

Single Units:

Spontaneous unit activity was sampled at 19000 Hz, amplified 10000 - 20000x and bandpass filtered between 600 Hz - 3000 Hz. Thresholds were set on the oscilloscope trace to capture unit waveforms that had at least a 3-to-1 signal-to-noise ratio. The unit clusters were cut offline using a template matching protocol, and occasionally scanned manually to discard any artifacts that were missed by the template cut. Peri-event time histograms with 10 second bins and autocorrelations (-1 to +1 seconds with 1 ms bins) for individual units were generated using Brainwave. The average baseline rate of the units was calculated by dividing the total number of spikes (indicated in the peak of the autocorrelation) in the control period by the total number of seconds. Average waveforms and autocorrelations were performed for the 5 min. control period and for a 5 min. period near the end of the record to ensure that the same unit was being recorded both at the beginning and the end of the experiment. If the autocorrelations suggested a bursting cell, the unit record was examined for doublet waveforms to confirm that the classification was not an artifact

of a noisy baseline.

Filtered action potential widths were measured as the time between the maximum and minimum point of the unit action potential waveform (see Jung and McNaughton, 1993; Mizumori et al., 1989).

EEG:

Hippocampal EEG was digitized at 200 Hz and sampled in 5 second epochs. This signal was amplified 50x and bandpass filtered from 0.1 - 100 Hz. Initially, records before and after the glutamate ejection were assessed visually for every 5 sec. bin. While this suggested that theta occurred after the flag, a more quantitative approach seemed desirable. The Brainwave FFT analysis program was then utilized to assess maximum power and the power spectrum in some records. The original data points had not been collected in a power of 2, it was necessary to pad every 1000 points with 24 zero points to make the total number a power of 2 (1024). The actual analysis was performed on 512 point bins (splitting the 1024 pt. bins in half) so every other bin was the original and contained only the original points. This provided a frequency at maximum power for every 2.5 s.

Brains were removed and frozen at the end of each experiment. Cerebral hemispheres were sectioned coronally at 40 μm. through the DG recording area to locate the pipette tip histologically. The cerebellum/brainstem was sectioned sagitally for verification of dye ejection and LC placement. Tracings of dye marked (and electrolytic lesioned) sites were made using a projection microscope. Tissue was then stained with 2.5% cresyl violet. Alternate sections taken through the DG were reacted for glycogen phosphorylase enzyme histochemistry (Harley and Bielajew, 1992). The histochemical stain aided in localizing recording pipette tracks and tips.

RESULTS

In all fourteen animals, the population spike amplitude was reliably enhanced following glutamate ejection in the LC as expected from earlier studies assessing LC-NE synaptic release in the DG. The average maximal potentiation across subjects was 177.4% of baseline and long term potentiation was seen in 6 animals with another animal showing a marginal long term effect. The average duration of the short term changes was 287 seconds (from 5 animals with complete records). As reported earlier (Harley and Sara, 1992), potentiation was delayed and typically not seen in the first 20 sec. following glutamate ejection. Individual EP characteristics and potentiation effects are summarized for every experiment in Table 1a.

Concomitant cellular recording revealed that the effects of LC-NE activation on DG single units could be grouped into five categories: immediate excitation (n=3), immediate strong inhibition (n=4), immediate moderate inhibition (n=2), delayed suppression (n=3) and unaffected (n=2). In one experiment, a second ejection was given to the same animal and the initial cell effects were replicated. A summary of individual cell characteristics and individual DG and LC histology is provided in Table 1b. The five categories of cell effects will be considered separately. The figures 5 to

Expmnt	EP characteristics		EPSP Effect			Spike Effect			EEG (theta)
	EPSP slpe (uV/us)	Spike (uV)	Max. % inc.	Delay (sec.)	Dur. (sec.)	Max.% inc.	delay (sec.)	Dur. (sec.)	
13-1	5234	3969.39	118	20	120	139	20	270	bef & aft flg no chnge then loss
17-3	8751	9192.799	112	10	30	150	20	300	In LIA
18-1	2208	2212.84	110	20	160	132	20	1100	bef & aft flg no chnge then loss
19-1	7395	6480.056	117	20	60	151	10	360	bef & aft flg no chnge then loss
20-1	5341	5577.14	115	10	30	204	10	1100	In LIA
27-3	8917	7295.595	117	0	70	167	20	220	bef & aft flg no chnge then loss
29-3	7688	6240.74	114	20	40	136	20	240	Incr in freq after flag ^ control
30-1	4035	7111.227	114	30	20	129	30	390	bef & aft flg no chnge then loss
32-2	6050	5903.573	118	0	20	128	20	70	Incr in freq after flag ^ control
33-1	7831	2901.987	114	10	40	194	20	1100	bef & aft flg no chnge then loss
38-1	6569.5	10834.4	No effect	N/A	N/A	129	20	1100	bef & aft flg no chnge then loss
38-2	7108	11866.1	No effect	N/A	N/A	118	20	250	bef flg then loss
39-1	5763	7201.096	No effect	N/A	N/A	167	20	600	In LIA
40-1	5207	7626.558	116	20	80	187	30	270	bef & aft flg no chnge then loss
42-1	6437	221.6046	112	0	10	530	20	900	Incr in freq after flag ^ control

Table #1a:EP, EPSP, and EEG data for individual experiments.

Expmnt	Cell Characteristics							LC location
	Width (µs.)	Burst	Act. on EPSP	Histology	Rate (Hz)	% change	Duration (sec.)	
13-1	376.5	−	Rising portion	ventral subgranular (zne 4)	4.5	0%	230	anterior LC
17-3	376.5	−	Rise & drop	subgranular (zne 4)	0.32	595%	20	80 µm medial
18-1	815.8	−	Not reliably	Hilus (zne 4)	0.82	0%	50	anterior LC
19-1	878.5	−	Not reliably	Lower gran lyr (zne 4)	2.06	72%	50	in LC
20-1	1129.5	−	N/A	Hilus (zne 4)	4.25	N/A	N/A	posterior LC
27-3	414	−	Rise & drop	Hilus (zne 4)	2.78	144%	30	posterior LC
29-3	690	+	Rise & drop	subgranular	3.12	0%	40	dorso-medial LC
30-1	368	−	Rising portion	subgranular (zone 3)	4.25	0%	195	posterior LC
32-2	586	−	Drop portion	ventral blde (zne 4)	1.44	0%	30	posterior LC
33-1	828	−	Drop portion	Hilus (zne 4)	3.68	0%	60	medial anterior LC
38-1	644	+	Rising portion	CA3 near hilus	1	0%	550	in LC
38-2	644	+	Rising portion	CA3 near hilus	1.54	0%	600	in LC
39-1	690	+	Not reliably	N/A	0.53	0%	375	posterior LC
40-1	759	+	Rising portion	Hilus (zone 4)	1.1	0%	140	anterior LC 120 µm lat.
42-1	368	−	Not reliably	subgranular	5.48	190%	30	in LC

Table #1b:Cell data and histology for individual experiments.

38 provide a graphical summary of unit waveforms, autocorrelations, and peri-event time histograms for each experiment. Concomitant popspike and EEG events are also presented.

Immediate Excitation:

The first group consists of cells that increased their firing rate immediately after LC activation.

17-3:

In experiment 17-3 the cell had an action potential width of 376.5 μs., did not burst, and had a baseline rate of 0.32 Hz. It had been observed to fire with a subthreshold PP stimulus and when the LC was activated, this cell responded with an increase in its firing rate from 0.32 Hz to 1.9 Hz (595% of baseline) which lasted for 20 seconds. This may be a biphasic effect because the cell returned to firing rates in the low range of the baseline period for a further 60 sec.

The popspike amplitude increase (150% of baseline) occurred 30 sec. after the ejection, and lasted for 300 sec. An early period of enhanced potentiation was similar to the period of depressed unit activity and lasted for 70 sec. Zero or very low values in the popspike record correspond to transient glitches in this and later figures.

The EEG trace of this experiment was dominated by lower frequencies and no theta activity was observed. There was no cell rhythmicity in the autocorrelation, but

Figure #5: Experiment 17-3. A. Peri-event time histogram of unit firing around ejection (arrow). B. Anatomical section showing pipette trajectory in LC (dot) and marker dye spot (B). C. averaged unit waveform. D. Autocorrelation for total record (1 ms bins). E. Transverse hippocampal section showing pipette tip location. F. Two superimposed, waveform averaged popspike traces, before flag (with amplitude markers) and after.

A

B

C

D

E

F→

56
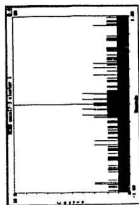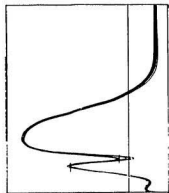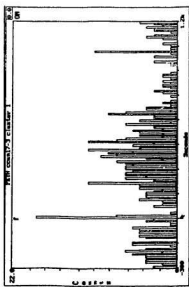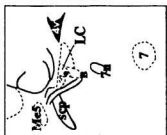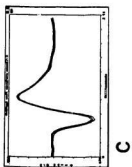
Figure #6: Experiment 17-3. A. Graph showing relationship of unit effects to popspike effects in time (arrow represents ejection). B. Graph of FFT analysis showing frequency at maximum power (arrow represents ejection).

A
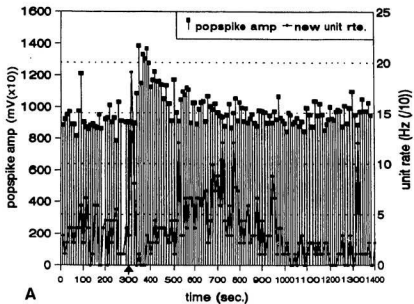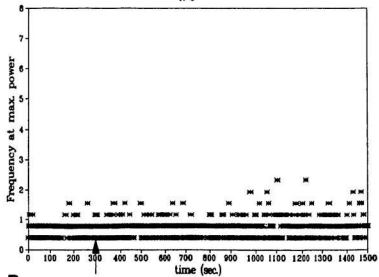
B

this could be due to the lack of theta EEG during the experiment.

This cell was found to be in the subgranular region of the hilus in the DG which is the same region where Pang and Rose found theta cells excited by NE. This may be a theta cell given its waveform and low firing rate in the absence of theta.

_42:1:_

This cell also had a narrow waveform, 368 μs., did not burst and had a baseline rate of 5.48 Hz. Immediately following LC activation, this cell increased its firing rate from 5.48 Hz to 9 Hz (190% of baseline) for 30 s. followed by a suppression for 120 s.

The popspike amplitude increase (530% of baseline) was delayed for 20 s., occurring 30 s. after the ejection and lasting for 900 s. which is considered a long term effect. The early phasic portion of the popspike increase (2 min. 30 s.) corresponded to the suppression of this unit's activity below baseline (2 min. 12 s.) after its phasic increase.

The FFT analysis showed a large amount of power in the theta frequency range with an increase in frequency (3.5 Hz to 6 Hz) within 20 s. after the flag. This corresponds to the unit increase, in that they both occur immediately after the flag and are relatively short lasting. There is a loss of the theta frequency after the

Figure #7: Experiment 42-1. A. Peri-event time histogram of unit firing around ejection (arrow). B. Anatomical section showing pipette trajectory in LC (dot) and marker dye spot (B). C. averaged unit waveform. D. Autocorrelation for total record (1 ms bins). E. Transverse hippocampal section showing pipette tip location. F. Two superimposed, waveform averaged popspike traces, before flag (with amplitude markers) and after.

A

B

C

D

E

F
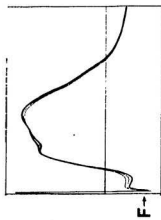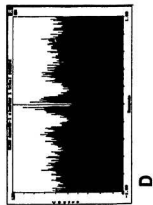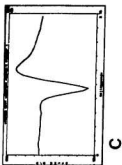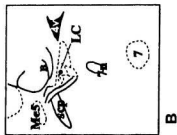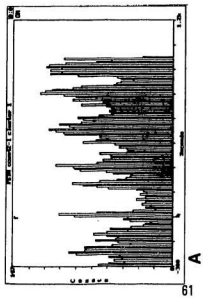
Figure #8: Experiment 42-1. A. Graph showing relationship of unit effects to popspike effects in time (arrow represents ejection). B. Graph of FFT analysis showing frequency at maximum power (arrow represents ejection).

A

B

63
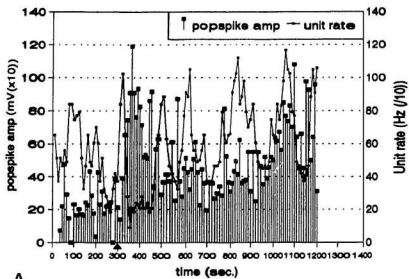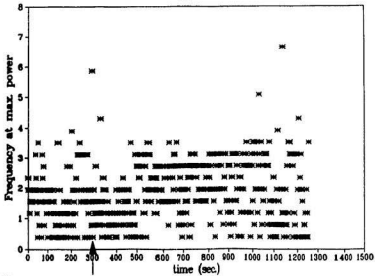
flag that lasts for 3 min. and 30 s. This loss only roughly corresponds with the suppression of cell activity and with the phasic portion of the popspike amplitude increase. The autocorrelation indicated a rhythmicity of about 3 Hz, which was the predominant rhythm observed in the FFT analysis.

This cell was also found in the subgranular region of the hilus and possesses characteristics common to the interneurons of that area namely, high baseline firing rate, rhythmicity, theta activity modulation and no bursts.

27:3:

Similar to the above cells, this cell has a width of 414 μs., a baseline firing rate of 2.78 Hz, and did not burst. After LC activation, this cell increased its rate from 2.78 Hz to 4 Hz (144% of baseline) for a period of 30 s. A return to a firing rate below baseline also occurred after the increase and lasted for the remainder of the record (record incomplete).

The characteristic popspike amplitude increase (max. 167%) was delayed 20 s., occurring 30 s. after the ejection and lasting for 220 s.

The FFT showed a flag related frequency increase in theta, within 20 s. after the flag it was within the range of control period theta frequencies. A second theta increase was seen approximately 40 s. after the flag, and was out of the

Figure #9: Experiment 27-3. A. Peri-event time histogram of unit firing around ejection (arrow). B. Anatomical section showing pipette trajectory in LC (dot) and marker dye spot (B). C. averaged unit waveform. D. Autocorrelation for total record (1 ms bins). E. Transverse hippocampal section showing pipette tip location. F. Two superimposed, waveform averaged popspike traces, before flag (with amplitude markers) and after.

A

B

MeS

LC

7

C

D

N.IX

E

F
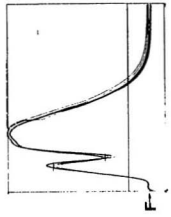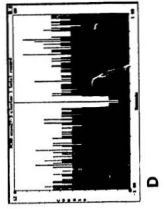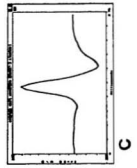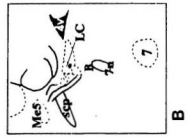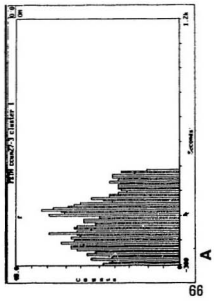
Figure #10: Experiment 27-3. A. Graph showing relationship of unit effects to popspike effects in time (arrow represents ejection). B. Graph of FFT analysis showing frequency at maximum power (arrow represants ejection).

A

27-3

B

68
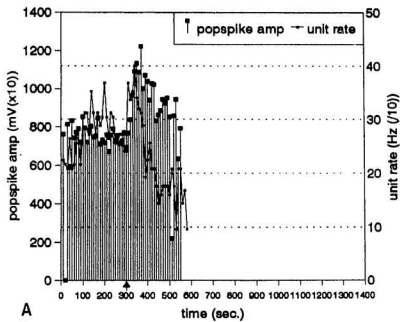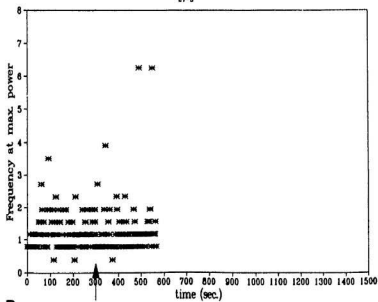
range of control period theta. These increases in theta frequency may relate to the unit activity increase but at the end of the record the theta frequency increases from 2.8 Hz to 6.5 Hz and the cell rate is not increased above baseline levels. The autocorrelation was not rhythmic.

This cell was not located anatomically. The cell has a relatively narrow waveform, possesses a moderately high firing rate and does not burst, but, the lack of rhythmicity and the lack of a clear relation between firing rate and theta, makes it difficult to classify as a theta cell.

Immediate Strong Inhibition:

This group consists of 4 animals where the recorded cells showed a strong, immediate inhibition following LC activation.

18-1:

This cell had a width of 815.8 μs., a baseline rate of 0.82 Hz, and did not burst. Following LC activation, there was an immediate decrease in cell activity (0% of baseline) from 0.82 Hz to 0 Hz and slightly above, for a duration of 50 s. The cell rate then returned to baseline levels.

The popspike amplitude increase (132%) occurred 20 s. after the flag and

Figure #11: Experiment 18-1. A. Peri-event time histogram of unit firing around ejection (arrow). B. Anatomical section showing LC placement (dot). C. averaged unit waveform. D. Autocorrelation for total record (1 ms bins). E. Transverse hippocampal section showing pipette tip location. F. Two superimposed, waveform averaged popspike traces, before flag (with amplitude markers) and after.
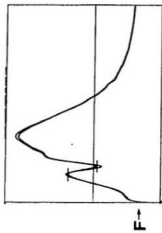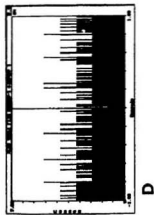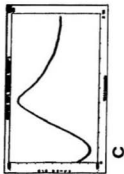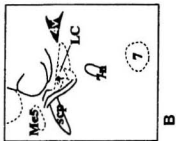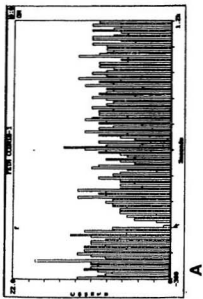
Figure #12: Experiment 18-1. A. Graph showing relationship of unit effects to popspike effects in time (arrow represents ejection). B. Graph of FFT analysis showing frequency at maximum power (arrow represents ejection).

A
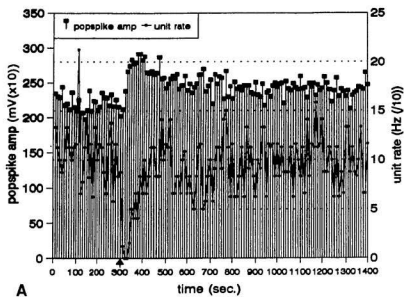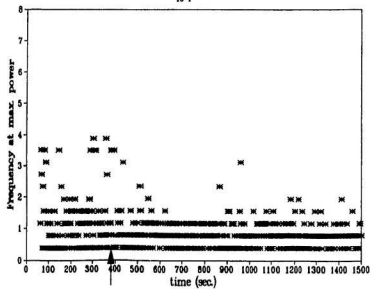
B

lasted for the duration of the experiment, which is considered a long term effect.

The FFT indicates some theta bins near the flag both just before and after. There was no ejection induced increase in theta frequency. Beginning 30 s. after the flag, there is a dropout of theta which lasts for 6 min. No correspondence was observed between the EEG and the unit record or the popspike record. The autocorrelation indicated only slight rhythmicity in the cell.

This cell was found in the hilus and the LC placement was anterior.

33-1:

Similarly, the width of this cell is 828 μs., with a baseline firing rate of 3.68 Hz, and no bursting. Immediately following LC activation, the cell rate decreases from 3.68 Hz to 0.4 Hz, then to 0 Hz (0% of baseline) for a period of 80 s. followed by a brief return to baseline and then a lowered spontaneous rate for the remainder of the record.

The popspike amplitude increase (194%) was delayed for 20 s., occurring 30 s. after the flag and lasting to the end of the record, and is considered long term. There was an early phasic increase in popspike amplitude which roughly, but not perfectly corresponded with the period of maximum suppression of the unit rate after the flag, lasting for 80 s.

Figure #13: Experiment 33-1. A. Peri-event time histogram of unit firing around ejection (arrow). B. Anatomical section showing pipette trajectory in LC (triangle) and marker dye spots (B). C. averaged unit waveform. D. Autocorrelation for total record (1 ms bins). E. Transverse hippocampal section showing pipette tip location. F. Two superimposed, waveform averaged popspike traces, before flag (with amplitude markers) and after.

A

B

C

D

E

F—

MeS

SCP

LC

PETH COUNTS / Cluster 1
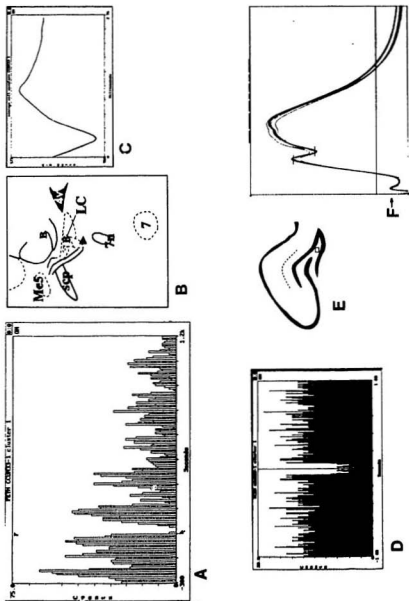
Figure #14: Experiment 33-1. A. Graph showing relationship of unit effects to popspike effects in time (arrow represents ejection). B. Graph of FFT analysis showing frequency at maximum power (arrow represents ejection).

A

B
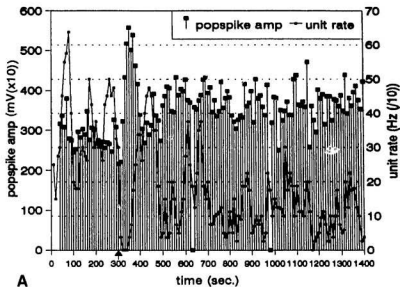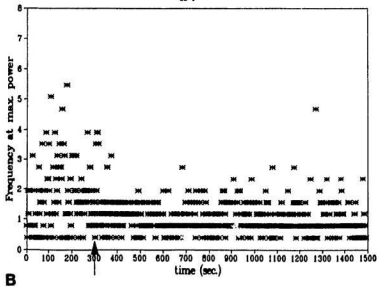
FFT analysis showed that low frequencies predominated within 20 s. after the flag. There were theta bins immediately following the flag, but they were not out of the range of those in the control period. The persistent low frequency rhythms remained constant for the remainder of the record. The autocorrelation showed mild rhythmicity.

This cell was found in the hilus.

32-2:

This cell had a width of 586 μs., a baseline firing rate of 1.44 Hz, and did not burst. When the LC was activated, the cell responded with immediate inhibition from 1.44 Hz to 0.3 Hz to 0 Hz (0% of baseline) which lasted for 30 s. There is a post-inhibition increase in firing rate above baseline levels and this settles into a stable firing rate which remains above control levels.

The popspike amplitude increase (max. 128%) was delayed by 20 s., occurred 30 s. after the flag and lasted for 70 s.

The FFT analysis indicates that there are 2 bins within 20 s. after the flag which show increased theta frequency. Following this is a theta dropout period of 1 min. after which there is more sustained theta for the remainder of the record. This sustained theta may correspond to the cell maintaining a new higher baseline firing

Figure #15: Experiment 32-2. A. Peri-event time histogram of unit firing around ejection (arrow). B. Anatomical section showing pipette trajectory in LC (dot) and marker dye spot (B). C. averaged unit waveform. D. Autocorrelation for total record (1 ms bins). E. Transverse hippocampal section showing pipette tip location. F. Two superimposed, waveform averaged popspike traces, before flag (with amplitude markers) and after.
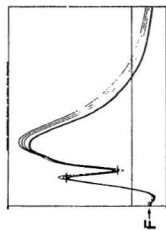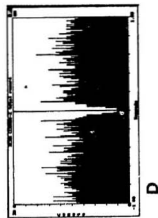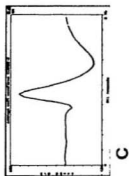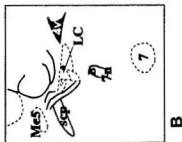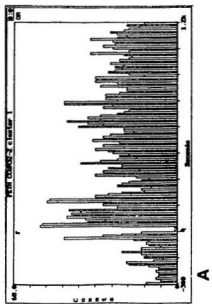
Figure #16: Experiment 32-2. A. Graph showing relationship of unit effects to popspike effects in time (arrow represents ejection). B. Graph of FFT analysis showing frequency at maximum power (arrow represents ejection).

A
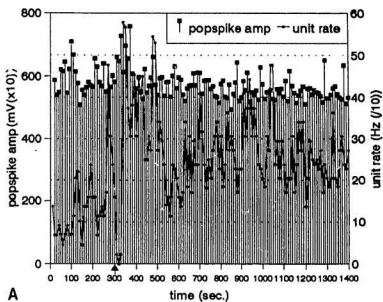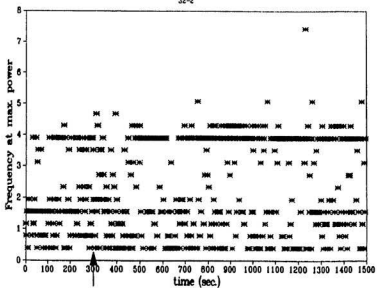
B

rate. However, there is also correspondence between the immediate inhibition of the

'' and the immediate increase in theta frequency in the bins after the flag. The autocorrelation did not show rhythmicity.

This cell was found in the hilus near the ventral blade of the DG.

13-1:

The width of this cell was 376.5 μs., it had a baseline firing rate of 4.5 Hz, and did not burst. Following LC activation, this cell responded immediately with inhibition of its firing rate from 4.5 Hz to 0 Hz (0%) and just above for 230 s. The cell then returned to its original baseline firing rate.

The popspike amplitude increase (139%) was delayed for 20 s., occurred 30 s. after the flag and lasted for 270 s. This short term increase outlasts the cell inhibition but again, the early stronger potentiation appeared to correspond to the duration of the cell inhibition.

The FFT analysis showed some scattered theta related bins near the flag, but no flag induced effects. There seemed to be no theta modulation of the unit in this record. The autocorrelation showed only mild rhythmicity.

This cell was found in the subgranular layer of the ventral blade of the DG.

Figure #17: Experiment 13-1. A. Rate-meter time histogram of unit firing around ejection (arrow) (standard peri-event histogram not available). B. Anatomical section showing LC placement (dot). C. averaged unit waveform. D. Autocorrelation for total record (1 ms bins). E. Transverse hippocampal section showing pipette tip location. F. Two superimposed, waveform averaged popspike traces, before flag (with amplitude markers) and after.
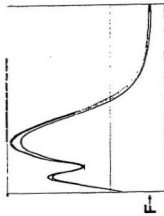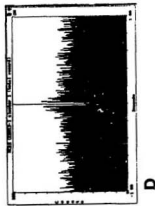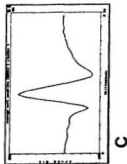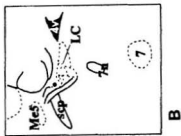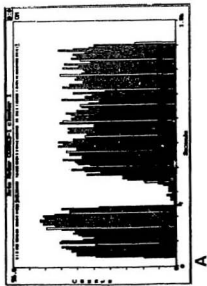
Figure #18: Experiment 13-1. A. Graph showing relationship of unit effects to popspike effects in time (arrow represents ejection). B. Graph of FFT analysis showing frequency at maximum power (arrow represents ejection).

A
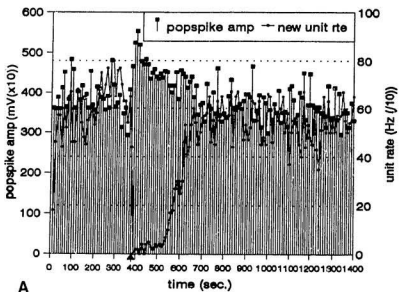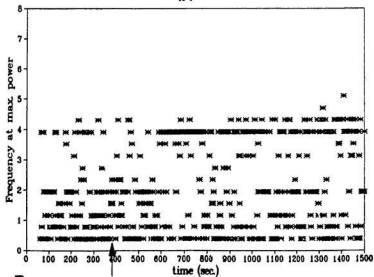
B

Immediate Moderate Inhibition:

The 2 cells in this group showed immediate, but only moderate inhibition of cell activity following LC activation.

19-1:

This cell had a width of 878.5 μs., a baseline firing rate of 2.06 Hz, and did not burst. Following LC activation, the cell rate was inhibited from 2.06 Hz to 1.5 Hz (72% of baseline) for a period of 50 s. The firing rate then returned to baseline briefly and then fell to a level below the control period.

The popspike amplitude increase (max. 151%) was delayed for 10 s., occurring 20 s. after the flag and lasting for 360 s. which was the end of the record. A long term effect could not be evaluated. No clear correspondence between the unit and popspike effect was evident.

The FFT analysis showed one bin of increased theta frequency within 20 s. after the flag. This increase, however, is not outside control levels. There is no evidence of any other correspondence between theta and the other effects. The autocorrelation showed no rhythmicity.

This cell was found in the subgranular layer of the hilus and its LC placement was in the body of the LC. However, due to the short record, conclusions could not

Figure #19: Experiment 19-1. A. Peri-event time histogram of unit firing around ejection (arrow). B. Anatomical section showing LC placement (dot). C. averaged unit waveform. D. Autocorrelation for total record (1 ms bins). E. Transverse hippocampal section showing pipette tip location. F. Two superimposed, waveform averaged popspike traces, before flag (with amplitude markers) and after.
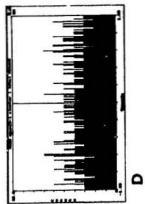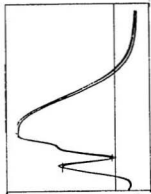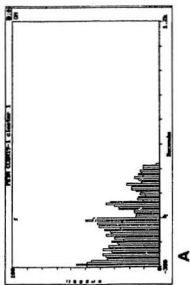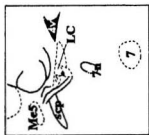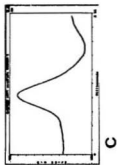
Figure #20: Experiment 19-1. A. Graph showing relationship of unit effects to popspike effects in time (arrow represents ejection). B. Graph of FFT analysis showing frequency at maximum power (arrow represents ejection).

A
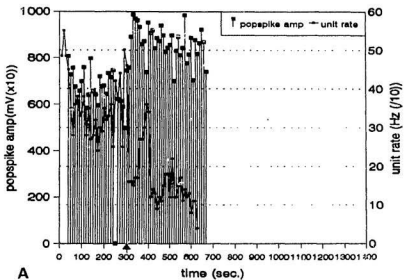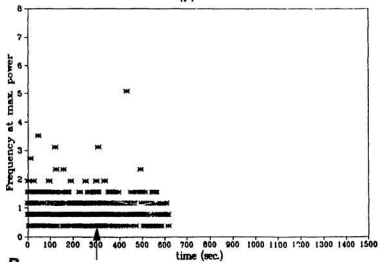
B

be reached about long term effects.

40-1:

The recorded cell width was 759 μs., the baseline firing rate was 1.1 Hz, and it burst. LC activation caused an immediate, but moderate decrease in cell firing rate from 1.1 Hz to 0.35 Hz (0%) which lasted for 140 s. The cell then returned to a firing rate which was higher than the control period rate for the remainder of the record.

The characteristic popspike amplitude increase (max. 187%) was delayed for 30 s., occurring 40 s. after the flag and lasting for the total record, which is a long term effect. The phasic portion of the popspike increase (110 s.) corresponded approximately with the unit inhibition.

The FFT analysis showed an increased variability in theta frequency after ejection together with more bins in the 2 - 3 Hz range. A loss of theta occurred 50 s. after the flag and returned only briefly in two bins through to the end of the record. The dominance by lower frequencies was seen about the same time as the unit achieved a higher baseline. No rhythmicity was observed in the autocorrelation.

This cell was found in the hilus.

Figure #21: Experiment 40-1. A. Peri-event time histogram of unit firing around ejection (arrow). B. Anatomical section showing pipette trajectory in LC (dot) and marker dye spot (B). C. averaged unit waveform. D. Autocorrelation for total record (1 ms bins). E. Transverse hippocampal section showing pipette tip location. F. Two superimposed, waveform averaged popspike traces, before flag (with amplitude markers) and after.
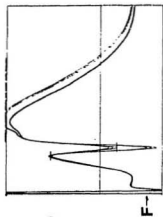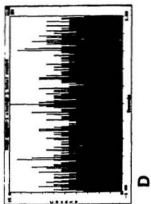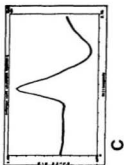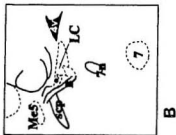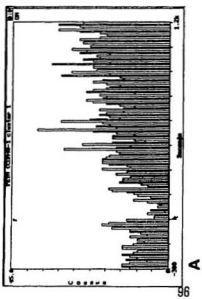
Figure #22: Experiment 40-1. A. Graph showing relationship of unit effects to popspike effects in time (arrow represents ejection). B. Graph of FFT analysis showing frequency at maximum power (arrow represents ejection).

A

B
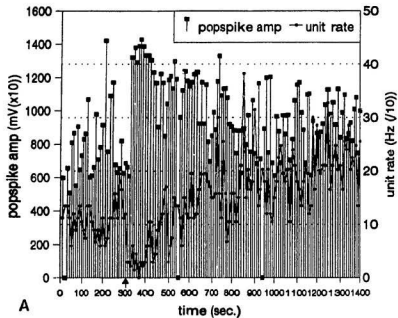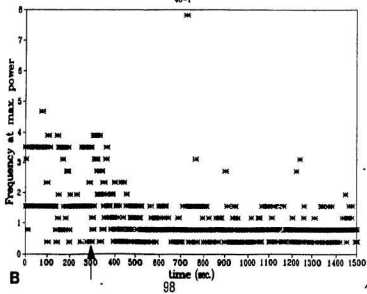
Delayed Suppression:

The 3 cells in this group show a clear delay to changes in firing after LC activation.

_39·1:_

This cell had a width of 690 μs., a baseline firing rate of 0.53 Hz, and it burst. Following LC activation, the inhibition did not take place until 10 seconds after the flag when the rate decreased from 0.53 Hz to 0 Hz (0%) for 375 s. The cell returned to a baseline which was higher than the control period.

The popspike increase (167%) was delayed for 20 s., occurred 30 s. after the flag and lasted for 600 s. and then returned to baseline. There was no correspondence between the unit changes and the popspike change.

FFT analysis revealed a small increase in low frequency activity for one bin within 20 s. after the flag. There was one bin of theta seen 3 min. after the flag which did not correspond to any of the other measures. An increase in low frequencies was seen at the end of the record and may coincide with the increased baseline firing rate of the cell. No rhythmicity was seen in the autocorrelation.

The cell placement was not available.

Figure #23: Experiment 39-1. A. Peri-event time histogram of unit firing around ejection (arrow). B. Anatomical section showing LC pipette placement (dot). C. averaged unit waveform. D. Autocorrelation for total record (1 ms bins). E. Transverse hippocampal section showing pipette tip location. F. Two superimposed, waveform averaged popspike traces, before flag (with amplitude markers) and after.

101
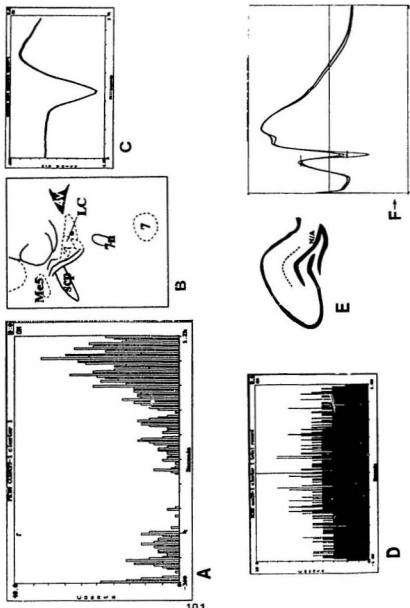
Figure #24: Experiment 39-1. A. Graph showing relationship of unit effects to popspike effects in time (arrow represents ejection). B. Graph of FFT analysis showing frequency at maximum power (arrow represents ejection).

A

B

103

38-1:
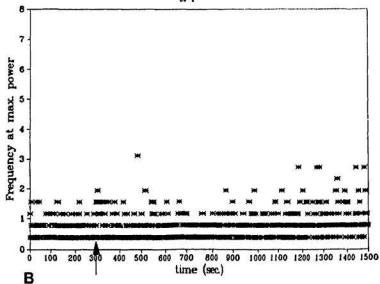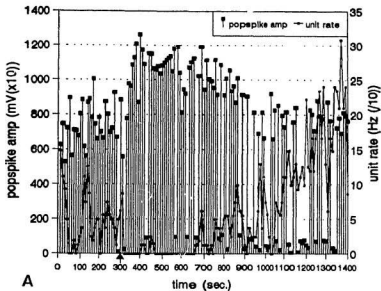
This cell had a width of 644 μs., a baseline firing rate of 1 Hz, and burst. Following LC activation, this cell decreased its rate with a delay of 10 s. from 1 Hz to 0 Hz (0%) for 550 s. The cell then returned, with increased variability, to control level firing rates. Another bursting cell recorded at the same time, from the same electrode, was not affected by the LC activation.

The popspike amplitude increase (max. 129%) was delayed for 20 s., occurred 30 s. after the flag and lasted for the remainder of the record, a long term effect. The unit change did not coincide with any portion of the spike effect.

FFT analysis revealed a distinct inhibition of the theta frequency immediately after the flag. The theta rhythm was inhibited for the remainder of the record. While LIA coincided with the long term popspike effect, no correspondence was observed with the unit effects. No rhythmicity was observed in the autocorrelations for the two unit clusters.

The cell was found in $CA3_c$.

38-2:

Experiment 38-2 was a replication of 38-1, except the electrode was moved

Figure #25: Experiment 38-1. A. Peri-event time histogram of unit firing around ejection (arrow). B. Anatomical section showing LC pipette placement (dot). C. averaged unit waveform. D. Autocorrelation for total record (1 ms bins). E. Transverse hippocampal section showing pipette tip location. F. Two superimposed, waveform averaged popspike traces, before flag (with amplitude markers) and after.
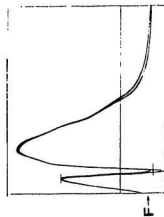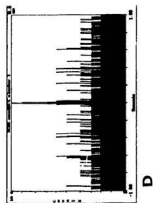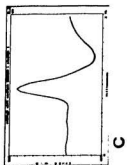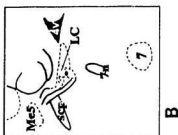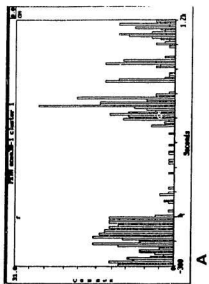
Figure #26: Experiment 38-1. A. Graph showing relationship of unit effects to popspike effects in time (arrow represents ejection). B. Graph of FFT analysis showing frequency at maximum power (arrow represents ejection).

A
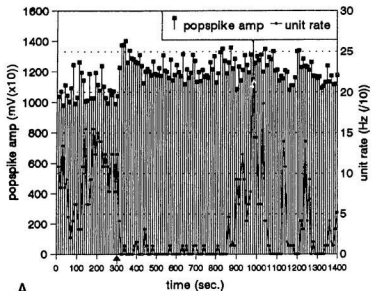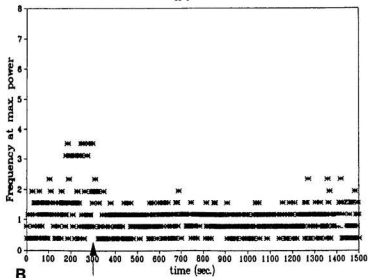
B

Figure #27: Experiment 38-2. A. Peri-event time histogram of unit firing around ejection (arrow). B. Anatomical section showing LC pipette placement (dot). C. averaged unit waveform. D. Autocorrelation for total record (1 ms bins). E. Transverse hippocampal section showing pipette tip location. F. Two superimposed, waveform averaged popspike traces, before flag (with amplitude markers) and after.
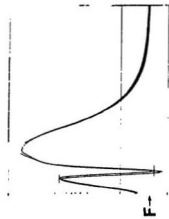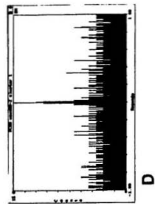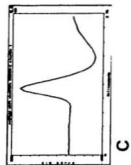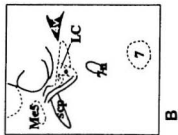
Figure #28: Experiment 38-2. A. Graph showing relationship of unit effects to popspike effects in time (arrow represents ejection). B. Graph of FFT analysis showing frequency at maximum power (arrow represents ejection).
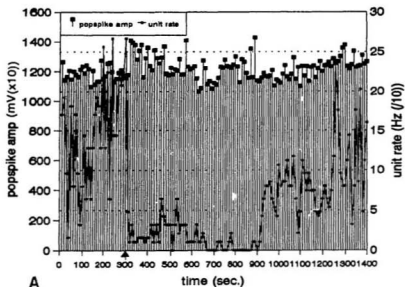
A
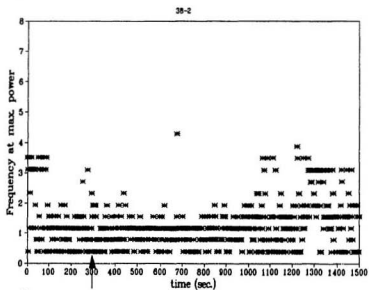
B

ventral approximately 100 μm. and two cells were again seen and monitored during a second glutamate ejection. As in 38-1, the cell width was 644 μs. and its rate was 1.54 Hz with bursting. The cell inhibition effect occurred with a delay of 10 s. after the flag, lasting for 10 min.. Another bursting cell was recorded which showed no effect upon LC activation.

The popspike amplitude increase (max. 118%) was delayed for 20 s., occurred 30 s. after the flag and lasted for 250 s. Although this was a short-term change, the earlier long-term change was still present.

The FFT analysis showed a loss of theta occurring immediately after the flag lasting for 10 min. with a return to theta after this period. The autocorrelation of both cells showed no rhythmicity.

28-3:

The recorded cell width was 690 μs., the baseline firing rate was 3.12 Hz, and the cell burst. Following LC activation, there was a delay of 10 s. before the actual cell effect took place. The cell rate decreased from 3.12 Hz to 0 Hz (0%) for 40 s. The cell then returned to a baseline higher than control levels for 3 minutes and then settled to baseline levels of firing.

The popspike increase (max. 136%) was delayed for 20 s., occurred 30 s.

Figure #29: Experiment 29-3. A. Peri-event time histogram of unit firing around ejection (arrow). B. Anatomical section showing pipette trajectory in LC (dot) and marker dye spot (B). C. averaged unit waveform. D. Autocorrelation for total record (1 ms bins). E. Transverse hippocampal section showing pipette tip location. F. Two superimposed, waveform averaged popspike traces, before flag (with amplitude markers) and after.
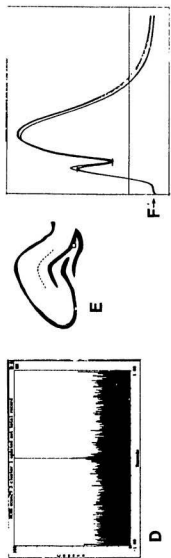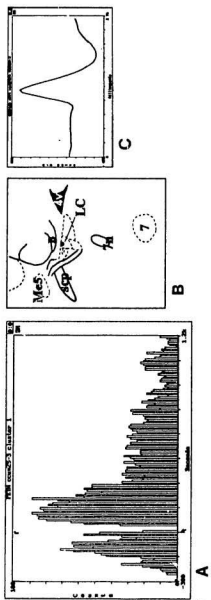
Figure #30: Experiment 29-3. A. Graph showing relationship of unit effects to popspike effects in time (arrow represents ejection). B. Graph of FFT analysis showing frequency at maximum power (arrow represents ejection).

A

B

117
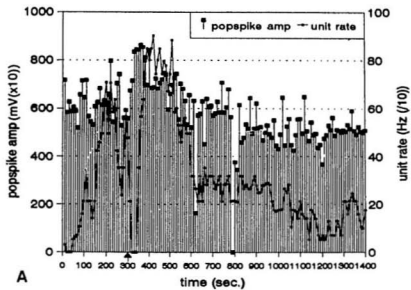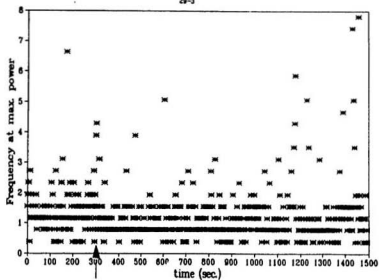
after the flag and lasted 240 s. The initial phasic increase in the popspike amplitude (70 s.) coincided with the inhibition of the cell when including cell rate bins which were involved in the transition from the inhibition to the excitation.

FFT analysis revealed three increased frequency theta bins within 30 s. after the flag. these coincide closely with the inhibition phase of the cell effect. There is little theta observed starting 50 s. after the flag with only 3 bins reaching the theta level over 12 min. A return to theta with increased frequencies was observed towards the end of the record. There is no correspondence between this effect and the unit or popspike. The autocorrelation showed no rhythmicity.

This unit was found in the subgranular layer of the hilus.

Unaffected Cells:

30-1:

One cell, 30-1 (width : 368 μs., rate : 4.25 Hz, nonbursting), was not affected by LC activation. It was strongly theta rhythmic and decreased its rate 30 s. after the flag, coincident with the loss of theta power in the EEG for a duration of 250 s., after which, the EEG returned to a strong theta rhythm and the cell returned to a higher baseline level.

Figure #31: Experiment 30-1. A. Peri-event time histogram of unit firing around ejection (arrow). B. Anatomical section showing pipette trajectory in LC (dot) and marker dye spot (B). C. averaged unit waveform. D. Autocorrelation for total record (1 ms bins). E. Transverse hippocampal section showing pipette tip location. F. Two superimposed, waveform averaged popspike traces, before flag (with amplitude markers) and after.

A

B

C

D

E

F→

Mes

LC
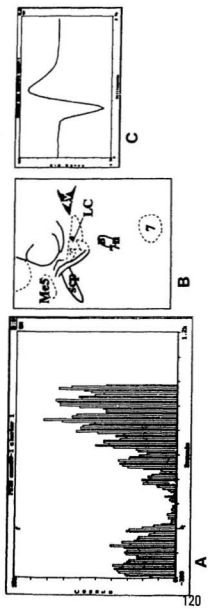
Figure #32: Experiment 30-1. A. Graph showing relationship of unit effects to popspike effects in time (arrow represents ejection). B. Graph of FFT analysis showing frequency at maximum power (arrow represents ejection).

A

B

122
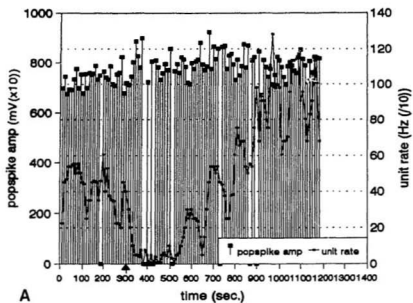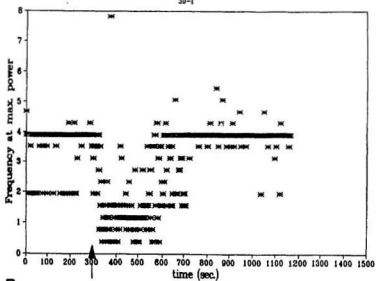
The popspike increase was delayed for 30 s., occurred 40 s. after the flag and lasted for the remainder of the record, in what was referred to as a marginal long term effect, due to large amplitude variability. There was no coincidence between the unit changes and the popspike change.

The FFT analysis showed a distinct theta inhibition occurring at 30 s. after the flag and lasting for 250 s. before coming back to strong theta. There is a direct correspondence between the theta and cell effect. Towards the end of the record, there are further increases in the theta frequency and this may correspond to the higher baseline rate of the cell at that time. The autocorrelation revealed a strong rhythmicity in the theta range.

This cell was found on the lateral edge of the subgranular layer.

Cell 2 in 38-1 and 38-2:

38-1:

This cell had a width of 644 μs., a baseline rate of 0.95 Hz, and burst. Following LC activation, there was no effect on this cell.

The popspike change and FFT analysis are the same as 38-1 in the delayed suppression section.

Figure #33: Experiment 38-1. A. Peri-event time histogram of unit firing around ejection (arrow). B. Anatomical section showing LC placement (dot). C. averaged unit waveform. D. Autocorrelation for total record (1 ms bins). E. Transverse hippocampal section showing pipette tip location. F. Two superimposed, waveform averaged popspike traces, before flag (with amplitude markers) and after.

C

MeS

LC

7

B

F→

E

A

D

125
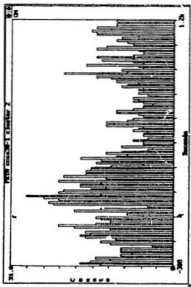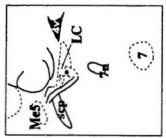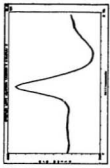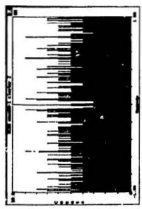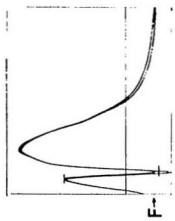
Figure #34: Experiment 38-1. A. Graph showing relationship of unit effects to popspike effects in time (arrow represents ejection). B. Graph of FFT analysis showing frequency at maximum power (arrow represents ejection).

A
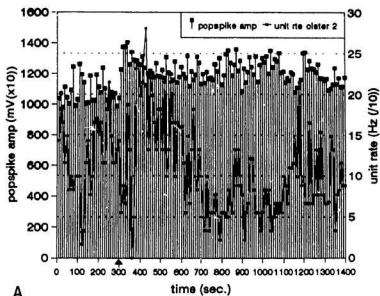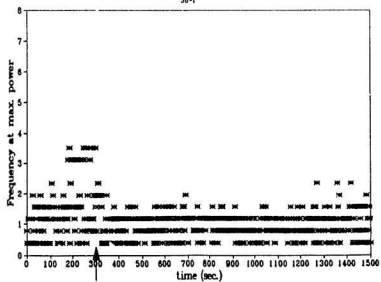
B

127

38-2:

This was the replication of experiment 38-1. The cell had the same characteristics as above and was not affected by LC activation.

The popspike change and FFT analysis are the same as 38-2 in the delayed suppression section.

20-1:

The unit record for this experiment was not clean and cell data were not successfully extracted from it. The spike increase (max. 204%) was pronounced, occurring 10 sec. after the flag and lasting for the duration of the record. which is a long term effect.

This occurred with an EEG record predominantly in LIA.

Evoked Firing:

75 % of all units, both bursting and nonbursting could be activated by PP stimuli subthreshold for a popspike. This suggests many of these cells may be participating in feedforward control of the DG circuit.

Figure #35: Experiment 38-2. A. Peri-event time histogram of unit firing around ejection (arrow). B. Anatomical section showing LC placement (dot). C. averaged unit waveform. D. Autocorrelation for total record (1 ms bins). E. Transverse hippocampal section showing pipette tip location. F. Two superimposed, waveform averaged popspike traces, before flag (with amplitude markers) and after.
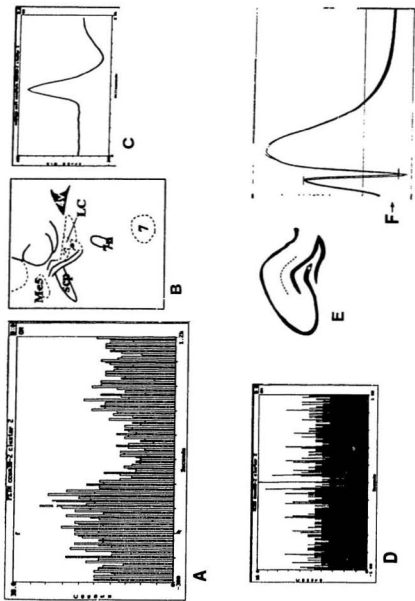
Figure #36: Experiment 38-2. A. Graph showing relationship of unit effects to popspike effects in time (arrow represents ejection). B. Graph of FFT analysis showing frequency at maximum power (arrow represents ejection).
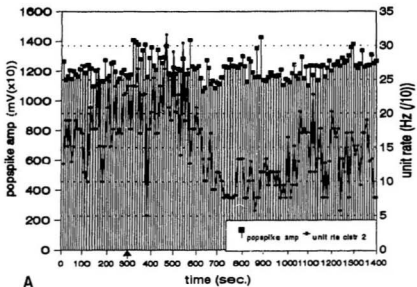
A
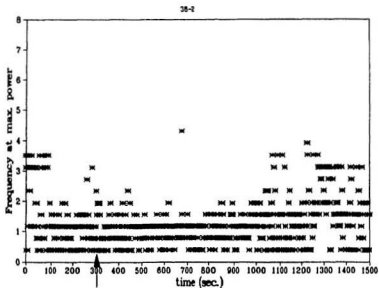
B

Figure #37: Experiment 20-1. A. Two superimposed, waveform averaged popspike traces, before flag (with amplitude markers) and after. B. Anatomical section showing pipette trajectory in LC (dot) and marker dye spot (B) C. Transverse hippocampal section showing pipette tip location.
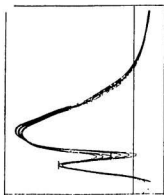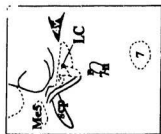
A
B
C

Figure #38: Experiment 20-1. A. Graph showing relationship of unit effects to popspike effects in time (arrow represents ejection). B. Graph of FFT analysis showing frequency at maximum power (arrow represents ejection).

A

B

136
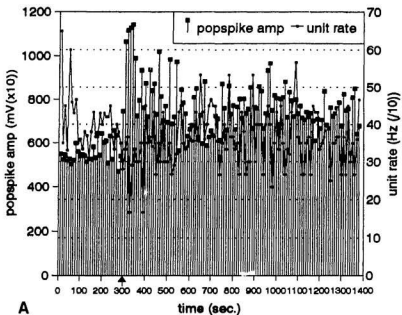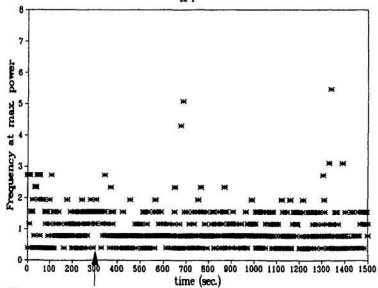
Theta results:

In 11 animals, there were theta bins within the 20 sec. period after the flag. There was a high incidence of theta episodes in the control period of 9 of these animals, while 2 showed a moderate to low incidence. In 2 of the 9 animals LC activation increased the theta frequency outside control ranges. One of the 9 showed a theta increase outside all of the control range except one bin. The three remaining animals of the total of 14, were in LIA for most of the record. Of the 9 animals with control theta, 8 showed a decrease in the theta frequency beginning an average of 32.5 seconds after the flag and lasting for an average of 6.27 min. The two with moderate to low incidence of theta and short records showed no change. One animal with strong theta before and after the flag also showed no change.

DISCUSSION

The concern of this study was to assess the effect of synaptic NE release in the DG by simultaneously monitoring changes in the PP-EP, the single unit activity of neurons at the same site, and the DG EEG. Potentiation of the population spike was used as evidence of successful activation of LC-NE release by local LC glutamate ejection. The ejection event itself was flagged in the recording records. As reported earlier, activation of LC produced consistent potentiation of the popspike amplitude which was typically delayed by 20 s. relative to LC activation. Effects in the cell circuitry were usually immediate when they occurred and theta EEG was often seen prior to the population spike change.

LC-NE: What Happens in LC:

It became evident after looking at the results of LC activation that the specific activation profile, with its various components, was important. Harley and Sara (1992) reported that following LC glutamate ejections, the LC immediately increases its firing rate from a normal 0.5- 1.5 Hz to a higher level of firing for a period of 250-400 ms. The activated rate is likely to be maximal for LC since firing in their 10 s. bin was

over 4 Hz. and the increase would have occurred only in the first 0.5 s. Following this rush of activity, a prolonged and complete suppression of LC cell firing was observed. The suppression typically lasted for an average of 4-5 min. LC cells then returned to normal firing rate. These three components, immediate short excitation, abrupt and prolonged suppression, and return to normal rate, appear to be factors in the mediation of cell effects in the present study.

LC-NE and Single Units:

Nonbursting cells:

It has been shown that non-bursting cells in the DG have interneuron characteristics in that they are all likely GABAergic (Seress and Ribak, 1983). Such cells are concentrated in the subgranular zone (Ribak and Seress, 1983; Buckmaster and Schwartzkroin, 1995), a region previously shown to have the densest NE innervation from LC (Koda et al., 1977 &78; Crutcher and Davis, 1980). In addition to nonbursting, a second electrophysiological characteristic for GABAergic interneurons is their typically narrow action potential waveforms ranging from $200 - 400$ μs. (Mizumori et al, 1989; Jung and McNaughton, 1993; Pang and Rose, 1987). It was

among cells of this type that immediate changes in firing occurred with LC-NE activation.

In previous work, NE had been reported variously to induce excitation or inhibition of the spontaneous activity of nonbursting DG cells in in vivo experiments (Segal et al., 1974a&b-76a&b; Pang and Rose 1987; Rose and Pang, 1989). In the present study, both excitation and inhibition were seen, but different subpopulations of cells appeared differentially involved in these effects.

Nonbursting neurons with narrow action potentials (368 - 414 μs.), which were in or near the subgranular zone (n=3) were immediately excited following LC activation. This group increased their firing rate for an average of 26.6 s. These results parallel those of Pang and Rose (1987) & Rose and Pang (1989) who recorded from interneurons in the subgranular region of the hilus and found the majority to be excited by iontophoresed NE. This parallel suggests the present effects are also produced by a direct action of LC-NE on these interneurons.

Nonbursting cells with wider action potentials (759-878 μs., n=4) and a scattered location in the hilus, showed immediate inhibition with LC activation lasting an average of 96 s. These results are analogous to those of Segal and Bloom (1974a&b-76a&b) who recorded from a variety of bursting and nonbursting cells in

140

Ammon's horn and the DG and found inhibition to be the characteristic effect when LC was electrically stimulated or NE was iontophoresed onto individual cells. While LC electrical stimulation may not have been as selective as LC glutamate, pharmacological controls used by Segal and Bloom and the parallel with NE iontophoretic effects suggest inhibition is also a direct effect of LC-NE actions on some GABAergic interneurons.

In the present study, two other nonbursting cells with narrow waveforms were affected differently than the main group. One was briefly and immediately inhibited by LC-NE as were the cells with wider waveforms, and one was unaffected. The unaffected cell (30-1) was particularly interesting as it was a clearly identified phasic theta cell with a distinctly rhythmic autocorrelation (3 Hz), but its rate changes followed EEG changes broadly and it was not directly influenced by LC activation.

To summarize, at least 3 groups of GABAergic interneurons may be distinguished by their differential response to LC-NE: (a). a narrow action potential group with excitation following LC-NE activation, lasting ~26 s., (b). a wide action potential cell group with inhibition of firing following LC-NE activation lasting ~96 s., and (c). a group that may be unaffected by LC-NE activation. The positive cell effects may be directly attributable to LC-NE release since they are seen immediately with LC

141

activation and have been observed to occur with local and direct NE application to nonbursting populations.

Bursting Cells:

Bursting cells are defined as cells which can fire groups of action potentials with less than 10 ms intervals (Fox and Ranck 1981). Pyramidal cells in the DG are found in layer $CA3_c$ and in the hilus (referred to as displaced pyramidal cells). Mossy cells, a glutamatergic interneuron type, may also be capable of bursts.

The main effect seen among bursting cells (n=3) in the present study was delayed suppression of activity. Bursting cells have wider action potentials than nonbursting interneurons (644 - 690 μs.). The delay averaged 10 s. after the flag and the suppression lasted for an average of 321 s. or about 5 min. Anatomically, some of these cells were in $CA3_c$ while other placements were more consistent with displaced pyramidal cells in the hilus. One neuron of this type (width: 759 μs.), showed an immediate, but mild suppression of activity lasting 140 s. The long-lasting and delayed suppression in activity seen among these cells may be related to the loss of tonic NE due to the delayed but prolonged suppression of the LC firing rate after the glutamatergic excitation since the time courses are quite similar.

Alternatively, Scanziani et al. (1993) have recently shown that NE decreases the amplitude of mossy fiber EPSP's in CA3 pyramidal cells and decreased pyramidal cell firing could be related to NE presynaptic modulation.

Proposed Model of Unit Effects:

Figure 39 summarizes these results. In the area of densest NE innervation, 3 interneuron subtypes are distinguished. Those nearest the subgranular layer, which may be basket cells, are either excited by or unaffected by LC activation, while others, located more distally and with wider waveforms are inhibited. the activity of some interneurons in this group have axons in the PP zone of the molecular layer. Bursting cells including those from $CA3_c$ are either unaffected or show prolonged reduced activity similar in length to the period of LC suppression. It is only in the zone of dense NE innervation that immediate effects are observed. This model of unit effects may account for several features of the spike amplitude modulation as described in the next section.

LC-NE and Spike Amplitude:

The population spike amplitude significantly increased with LC-NE in all
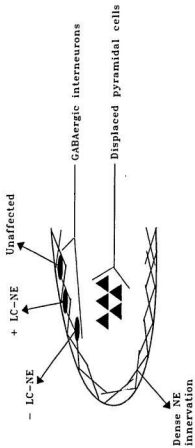
Figure #39. Diagram of proposed model of cell effects and interactions.

144

experiments. However, also present in all experiments was a time delay between the flag and the first potentiated spike which typically occurred at 30 s. after a delay of 20 s. Most cell changes were observed immediately after the flag.

The unit effects suggest one explanation of this delay. It is apparent from the immediate consequence of LC-NE release that one population of GABA cells is excited briefly while another is inhibited for a longer period. Two such changes in GABAergic influence could initially balance and prevent the appearance of a net increase in cell excitability. As the excitatory effect disappears, disinhibition should be evident. For example, in experiment 17-3, the cell excitation lasts 20 s. after the flag and the spike increase begins 20 s. after the flag. The longer inhibition of some interneurons would then contribute to, and may account for, the stronger, phasic increase in the popspike that is seen initially in all records. For example, in experiment 33-1, the cell is inhibited for 70 s. which corresponds to the initially stronger phasic increase in the popspike which ends 80 s. after the flag.

NE potentiation in 11/14 experiments continues beyond this phasic period however, suggesting a change in coupling of PP input to DG output is occurring and that NE potentiation is not simply a result of disinhibition as Buzsaki first hypothesized. GABAergic cell changes are transient relative to the overall potentiation.

A second explanation for the delay may simply be that there is a second messenger involved in mediating this effect and it takes a certain amount of time (on the order of seconds) to produce the effect. LTP itself has been shown to take ~30 s. to develop (Hanse and Gustafsson, 1992).

LC-NE and the EPSP:

An increase in the slope of the EPSP was observed in 12 of the 14 animals with an average onset of 14 s. after the flag. The average increase was 114.75% of baseline, and lasted 56.6 s. This EPSP effect was seen by analysing individually collected popspikes. Earlier studies (Neuman and Harley, 1983) that reported no EPSP changes may have missed these transient events by analysing averaged groups of EPs. A possible explanation for the present EPSP change may also be found in the single unit events. Inhibition of feedforward interneurons whose primary inhibitory target is the middle or outer molecular layer (Buckmaster and Schwartzkroin, 1995) might be predicted to alter the EPSP slope and amplitude. Dendritic disinhibition would be seen as a transient increase in the EPSP.

Dahl and Sarvey (1989) reported that NE can cause both long term EPSP and spike effects if the medial PP is stimulated selectively. However, the method used

here does not selectively activate one portion of the PP so the present transient EPSP effects probably differ from those observed by Dahl and Sarvey. Future in vivo studies are needed to verify that the medial PP EPSP shows long term potentiation.

LC-NE and EEG:

In the course of analysis of the EEG data, it became evident that using smaller bins (2.5 s.) for FFT analyses revealed transient NE effects which were often not observed in initial analyses using 5 s. bins. This may relate to the brief period of NE release activation.

NE was thought not to effect hippocampal theta until recently. The theta rhythm has been shown to be under cholinergic and serotonergic control (Vanderwolf, 1988). Robinson et al., (1977) did a study on whether the dorsal NE bundle projections from LC were linked to theta activity. They found that when the NE dorsal bundle connection was cut, the theta rhythm was still intact. However, it is possible that loss of brief phasic theta increases may have been overlooked.

Berridge and Foote, (1991) found tonic activation of LC with bethanecol, a cholinergic agonist, caused an increase in the relative power of theta compared to other frequencies in the EEG record. A delay of 5-30 s. after the start of the

increase in LC firing was observed to be the beginning of the effect period. Sainsbury et al., (1993) has also shown that detomidine, an $\alpha 2$ agonist, infused into the median raphe nucleus, will cause a release of type 2 theta (immobility theta). They suggest NE modulates serotonergic influences on the cholinergic system which in turn, influences theta.

In the present study, the relative power of theta was not measured. However, theta occurred after the flag in 11/14 animals which were in variable theta before the flag. Unlike Berridge and Foote, 3/11 animals in the present study showed increases in theta frequency outside the control range within 20 s. of the flag which are clearly ejection related. Three animals had predominantly LIA records and there was no flag related theta. This is consistent with Berridge and Foote's report that deeply anesthetised animals do not show LC-induced theta with bethanecol LC activation. In the present study, the LC was activated briefly and rapidly and the flag related theta was also brief and corresponding to the glutamate activation. Berridge and Foote's slow onset tonic change also appeared directly related to the LC firing pattern.

Eight animals which had frequent theta episodes prior to LC activation, subsequently showed a loss of theta frequencies beginning 30 s. after the ejection and lasting for an average of 6.7 min. This period of dominance by lower frequencies

148

may be explained in two ways. The characteristic and complete suppression of LC activity after the initial burst following glutamate ejection would cause a loss of tonic NE and this loss might produce the decrease in the incidence of theta. A recent paper by Berridge and Foote (1994) has shown that infusions of clonidine (35 nl or 150 nl) in the vicinity of the LC dramatically reduce theta frequency in the EEG. However, they only found this effect with bilateral LC suppression, not with unilateral suppression. The effect lasted for 30 - 180 min. and then the LC returned to baseline firing levels and the EEG returned to its previous theta frequency level. These findings are in close agreement to this study, except that here, unilateral LC suppression achieves similar results. Again, anesthetic level may be important, as subjects with the more consistent theta patterns showed only brief or no theta suppression after unilateral LC glutamate. Alternatively, theta may be overdriven by the initial strong NE release which can result in theta block (Vertes, 1980; Paiva et al., 1976).

Interrelationships Among EEG Changes & Changes in the other Variables:

The Relation of Cell Changes to EEG Changes:

Generally, with regard to cell activity in broad relation to the EEG, some cells

149

in this study may be loosely classified as phasic theta-on cells (42-1 and 30-1), tonic theta-off cells (40-1 and 29-3), or tonic theta-on cells (17-3, 38-2, 32-2 and 33-1).

However, the action of NE on these cells appears independent of its involvement in theta support. For example, the cell in experiment 32-2 appears to be a tonic theta-on cell, but when LC is activated, the cell is inhibited even in the presence of an increase in theta frequency outside the control range. Clearly there is a dissociation between LC-NE effects on the unit and effects on EEG.

The Relation of EEG to Popspike:

Greenstein et al. (1988) reported that long term potentiation in the DG is preferentially induced at theta rhythm periodicity. In the present study, theta was seen after the flag in 11 animals, and in 5/6 animals that had long-term changes. One animal in LIA also showed a long term potentiation. While it is clear that potentiation can occur with LIA or theta as the predominant EEG signature, the presence of theta after LC activation in less deeply anesthetised rats is compatible with the suggestion that LC promotes DG circuit plasticity in multiple ways.

Earlier studies have found spike amplitude potentiation (Harley and Milway, 1986; Lacaille and Harley, 1985; Stanton and Sarvey, 1985b) and both excitatory and inhibitory cell effects (Segal and Bloom, 1974-76; Pang and Rose, 1987; Rose and Pang, 1989) to be β-receptor mediated. More recent work has shown that NE effects on EEG are also β-receptor mediated (Berridge and Foote, 1991). Therefore, it is possible that all the LC-NE effects in this study are β-receptor mediated. However, presynaptic inhibition of mossy fiber glutamate release is reported to be α-mediated (Scanziani et al., 1993) and a re-examination of cell effects with pharmacological controls would be of interest.

Caveats:

Cell Identification:

While cells can be classified with a degree of certainty here based on their electrophysiological characteristics and location, to be certain of the cell type, intracellular recording followed by dye-filling the cell and locating it in the stained sections must be attempted. The present, surprising results are suggestive of discrete

and selective LC control of different GABAergic interneuron types presumably in the service of attentional and memorial processes, but such claims will require more challenging studies to verify this hypothesis.

LC Selectivity of Glutamate Application:

While it appeared that the deeper dye ejections were due to experimenter error, it is possible that in some experiments, activation effects were due to glutamate stimulation of other cell groups. However, previous studies with both EP and EEG changes (Harley and Milway, 1986; Berridge and Foote, 1994) suggest only LC ejections are likely to have given this profile of EP and EEG changes.

Conclusions:

The long term enhancement of the population spike has not specifically been accounted for by any one of the effects observed in this study. However, it seems that several conditions are being set up by LC-NE release which would act together with cellular events to promote the enduring increased coupling between PP input and granule cell output. The transient initial increases in theta may provide the synchronization for the initialization and maintenance of a long term circuitry change.

In addition, the inhibition of GABA interneurons would also provide favourable conditions for increased cellular excitability leading to a long term circuitry change. Finally, cyclic AMP may be involved in the actual coupling change itself. It seems that the role of NE in this system is to modulate several parameters which collectively act to promote long term enhancement of DG circuit throughput.

REFERENCES

Alexander, R.W., Davis, J.N., and Lefkowitz, R.J. (1975) Direct identification and characterisation of β-adrenergic receptors in rat brain. *Nature 258*: 437-440.

Amaral, D.G. (1978) A golgi study of cell types in the hilar region of the hippocampus in the rat. *J. Comp. Neur 182*: 851-914.

Amaral, D. G., and Woodward, D. J. (1977) A hippocampal interneuron observed in the inferior region. *Brain Research 124*: 225-236. Cited by: Amaral, D.G. (1978) A golgi study of cell types in the hilar region of the hippocampus in the rat. *J. Comp. Neur 182*: 851-914.

Andersen, P., Bliss, T. V. P., and Skrede, K. K. (1971) Unit analysis of hippocampal population spikes. *Experimental Brain Research 13*: 208-221.

Andersen, P., Holmqvist, B., and Voorhoeve, P. E. (1966) Entorhinal activation of dentate granule cells. *Acta Physiologica Scandinavica 66*: 448-460.

Andersen, P., and Loyning, Y. (1962) Interaction of various afferents on CA1 neurons and dentate granule cells. *Coll. int. C.N.R.S. 107*: 23-42. Cited by : Andersen, P., Holmqvist, B., and Voorhoeve, P. E. (1966) Entorhina' activation of dentate granule cells. *Acta Physiologica Scandinavica 66*: 448-460.

Armstrong-James, M., and Fox, K. (1983) Effects of iontophoresed noradrenaline on the spontaneous activity of neurones in rat primary somatosensory cortex. *Journal of Physiology 335*: 427-447.

Assaf, S. Y., and Miller, J. J. (1978) Neuronal transmission in the dentate gyrus: Role of inhibitory mechanisms. *Brain Research 151*: 587-592.

Berridge, C. W., and Foote, S. L. (1991) Effects of locus coeruleus activation on electroencephalographic activity in neocortex and hippocampus. *The Journal of Neuroscience 11(10)*: 3135-3145.

Berridge, C. W., and Foote, S. L. (1994) Locus coeruleus-induced modulation of

forebrain electroencephalographic (EEG) state in halothane anesthetized rat. *Brain Research Bulletin 35*: 597-605.

Blackstad, T. (1958) On the termination of some afferents to the hippocampus and fascia dentata. *Acta Anat. 35*: 202-214. Cited by : Andersen, P., Holmqvist, B., and Voorhoeve, P. E. (1966) Entorhinal activation of dentate granule cells. *Acta Physiologica Scandinavica 66*: 448-460.

Bland, B. H., Andersen, P., and Ganes, T. (1975) Two generators of hippocampal theta activity in rabbits. *Brain Research 94*: 199-218. Cited by Green, K. F., and Rawlins, J. N. P. (1979) Hippocampal theta in rats under urethane: generators and phase relations. *Electroencephalography and Clinical Neurophysiology 47*: 420-429.

Bland, B. H., Andersen, P., Ganes, T., and Sveen, O. (1980) Automated analysis of rhythmicity of physiologically identified hippocampal formation neurons. *Experimental Brain Research 38*: 205-219.

Bland, B. H., and Colom, L. V. (1989) Preliminary observations on the physiology and pharmacology of hippocampal theta-off cells. *Brain Research 505*: 333-336. Cited by Bland, B. H., and Colom, L. V. (1993) Extrinsic and intrinsic properties underlying oscillation and synchrony in limbic cortex. *Progress in Neurobiology 41*: 157-208.

Bland, B. H., and Wishaw, I. Q. (1976) Generators and topography of hippocampal theta (RSA) in the anesthetized and freely moving rat. *Brain Research 118*: 259-280. Cited by Green, K. F., and Rawlins, J. N. P.(1979) Hippocampal theta in rats under urethane: generators and phase relations. *Electroencephalography and Clinical Neurophysiology 47*: 420-429.

Buckmaster, P.S. and Schwartzkroin, P.A. (1995) Interneurons and inhibition in the dentate gyrus of the rat in vivo. *The Journal of Neuroscience 15(1)*: 774-789.

Burgard, E. C., Decker, G. , and Sarvey, J. M. (1989) NMDA receptor antagonists block norepinephrine-induced long- lasting potentiation and long-term potentiation in rat dentate gyrus. *Brain Research 482*: 351-355.

155

Buzsaki, G., and Eidelberg, E. (1983) Phase relations of hippocampal projection cells and interneurons to theta activity in the anesthetized rat. *Brain Research 266*: 334-339.

Buzsaki, G. (1984) Feed-forward inhibition in the hippocampal formation. *Progress in Neurobiology 22*: 131-153.

Buzsaki, G., Leung, L. S., and Vanderwolf, C. H. (1983) Cellular basis of hippocampal EEG in behaving rat. *Brain Research 6*:139-171. Cited by: Buzsaki, G. (1984) Feed-forward inhibition in the hippocampal formation. *Progress in Neurobiology 22*: 131-153.

Cedarbaum, J.M. and Aghajanian, G.K. (1976) Noradrenergic neurons of the locus coeruleus: inhibition by epinephrine and activation by the alpha-antagonist piperoxane. *Brain Research 112(2)*: 413-419.

Chetkovich, D. M., Gray, R., Johnston, D., and Sweatt, J. D. (1991) N-Methyl-D-aspartate receptor activation increases cAMP levels and voltage-gated Ca^{2+} channel activity in area CA1 of hippocampus. *Proc. Natl. Acad. Sci. USA 88*: 6467-6471.

Crutcher, K. A., and Davis, J. N. (1980) Hippocampal α- and β- adrenergic receptors: comparison of [3H]Dihydroalprenolol and [3H]WB 4101 binding with noradrenergic innervation in the rat. *Brain Research 182*: 107-117.

Dahl, D., and Sarvey, J. M. (1989) Norepinephrine induces pathway-specific long-lasting potentiation and depression in the hippocampal dentate gyrus. *Proceedings of the National Academy of Science. USA 86*: 4776-4780.

Fox, S. E., and Ranck, Jr., J. B. (1981) Electrophysiological characteristics of hippocampal complex-spike cells and theta cells. *Experimental Brain Research 41*: 399-410.

Freedman, R., Hoffer, B. J., Woodward, D. J., and Puro, D. (1977) Interaction of norepinephrine with cerebellar activity evoked by mossy and climbing fibers. *Experimental Neurology 55*: 269-288. Cited by Woodward, D. J., Moises, H. C.,

Waterhouse, B. D., Hoffer, B. J., and Freedman, R. (1979) Modulatory actions of norepinephrine in the central nervous system. *Federation Proc. 38*: 2109-2116.

Frizzell, L. M., and Harley, C. W. (1994) The N-Methyl-D-Aspartate channel blocker ketamine does not attenuate, but enhances, locus coeruleus- induced potentiation in rat dentate gyrus. *Brain Research 663*: 173-178.

Fujita, Y. (1962) Synaptic activation of dentate granule cells and its effect upon pyramidal cells in rabbit. *Coll. int. C.N.R.S. 107*: 47-68. Cited by : Andersen, P., Holmqvist, B., and Voorhoeve, P. E. (1966) Entorhinal activation of dentate granule cells. *Acta Physiologica Scandinavica 66*: 448-460.

Goodchild, A.K., Dampney, R.A.L., and Bandler, R. (1982) A method for evoking physiological responses by stimulation of cell bodies, but not axons of passage, within localized regions of the central nervous system. *Journal of Neuroscience Methods 6*: 351-363.

Gray, R. and Johnston, D. (1987) Noradrenaline and β-adrenoceptor agonists increase activity of voltage-dependent calcium channels in hippocampal neurons. *Nature 327*: 620-622.

Green, J. D., Maxwell, D. S., Schindler, W. J., and Stumpf, C. (1960) Rabbit EEG 'theta' rhythm: its anatomical source and relation to activity in single neurons. *Journal of Neurophysiology 23*: 403-420. Cited by Green, K. F., and Rawlins, J. N. P. (1979) Hippocampal theta in rats under urethane: generators and phase relations. *Electroencephalography and Clinical Neurophysiology 47*: 420-429.

Green, K. F., and Rawlins, J. N. P. (1979) Hippocampal theta in rats under urethane: generators and phase relations. *Electroencephalography and Clinical Neurophysiology 47*: 420-429.

Greenstein, Y. J., Pavlides, C., and Winson, J. (1988) Long-term potentiation in the dentate gyrus is preferentially induced at theta rhythm periodicity. *Brain Research 438*: 331-334.

Hanse, E., and Gustafsson, B. (1992) Long term potentiation and field EPSPs in the lateral and medial perforant paths in the dentate gyrus in vitro: a comparison. *European Journal of Neuroscience 4*: 1191-1201.

Harley, C.A. and Bielajew, C.H. (1992) Comparison of glycogen phosphorylase and cytochrome oxidase histochemical staining in rat brain. *Journal of Comparative Neurology 322(3)*: 377-89.

Harley, C. W., and Evans, S. (1988) Locus-coeruleus-induced enhancement of the perforant-path evoked potential: Effects of intradentate beta blockers. In: Woody, C.D., Alkon, D.L., McGaugh, J.L. (eds.). Cellular mechanisms of conditioning and behavioral plasticity. Plenum. New York. pp 415-423. Cited by Harley, C. W., and Sara, S. J. (1992) Locus coeruleus bursts induced by glutamate trigger delayed perforant path spike amplitude potentiation in the dentate gyrus. *Experimental Brain Research 89*: 581-587.

Harley, C. W., and Milway, J. S. (1986) Glutamate ejection in the locus coeruleus enhances the perforant path-evoked population spike in the dentate gyrus. *Experimental Brain Research 63*: 143-150.

Harley, C., Milway, J. S., and Lacaille, J-C. (1989) Locus coeruleus potentiation of dentate gyrus responses: evidence for two systems. *Brain Research Bulletin 22*: 643-650.

Harley, C. W., and Sara, S. J. (1992) Locus coeruleus bursts induced by glutamate trigger delayed perforant path spike amplitude potentiation in the dentate gyrus. *Experimental Brain Research 89*: 581-587.

Hendricks, C., and Teyler, T. J. (1983) Effects of blocking GABA on hippocampal CA1 inhibition and plasticity. *Society for Neuroscience abstracts 9*: 859. Cited by: Buzsaki, G. (1984) Feed-forward inhibition in the hippocampal formation. *Progress in Neurobiology 22*: 131-153.

Jung, M. W., and McNaughton, B. L. (1993) Spatial selectivity of unit activity in the hippocampal granular layer. *Hippocampus 3*: 165-182.

Koda, L. Y., and Bloom, F. E. (1977) A light and electron microscopic study of noradrenergic terminals in the rat dentate gyrus. *Brain Research 120*: 327-335.

Koda, L. Y., Wise, R. A., and Bloom, F. E. (1978) Light and electron microscopic changes in the rat dentate gyrus after lesions or stimulation of the ascending locus coeruleus pathway. *Brain Research 144*: 363-368.

Lacaille, J.-C., and Harley, C. W. (1985) The action of norepinephrine in the dentate gyrus: Beta-mediated facilitation of evoked potentials in vitro. *Brain Research 358*: 210-220.

Lacaille, J.-C., and Schwartzkroin, P.A. (1988) Intracellular responses of rat hippocampal granule cells in vitro to discrete applications of norepinephrine. *Neuroscience Letters 89*: 176-181.

Lynch, M.A. and Bliss, T.V.P. (1986) Noradrenaline modulates the release of [14C] glutamate from dentate but not from CA1/CA3 slices of rat hippocampus. *Neuropharmacology 25*: 171-176.

Madison, D.V. and Nicoll, R.A. (1986a) Actions of noradrenaline recorded intracellularly in rat hippocampal CA 1 pyramidal neurones, in vitro. *Journal of Physiology 372*: 221-244.

Madison, D.V. and Nicoll, R.A. (1986b) Cyclic adenosine 3', 5'-monophosphate mediates β-receptor actions of noradrenaline in rat hippocampal pyramidal cells. *Journal of Physiology 372*: 245-259.

Milner, T. A., and Bacon, C. E. (1989) GABAergic neurons in the rat hippocampal formation: ultrastructure and synaptic relationships with catecholaminergic terminals. *The Journal of Neuroscience 9(10)*: 3410-3427.

Mizumori, S. J. Y., Barnes, C. A., and McNaughton, B. L. (1989) Reversible inactivation of the medial septum: selective effects on the spontaneous unit activity of different hippocampal cell types. *Brain research 500*: 99-106.

Neuman, R. S., and Harley, C. W. (1983) Long-lasting potentiation of the dentate gyrus population spike by norepinephrine. *Brain Research 273*: 162-165.

Oleskevich, S., Descarries, L., and Lacaille, J. C. (1989) Quantified distribution of the noradrenaline innervation in the hippocampus of adult rat. *The Journal of Neuroscience 9(11)*: 3803-3815.

Paiva, T., Lopes Da Silva, F. H., and Mollevanger, W. (1976) Modulating systems of hippocampal EEG. *Electroencephalography and Clinical Neurophysiology 40*: 470-480.

Pang, K., and Rose, G. M. (1987) Differential effects of norepinephrine on hippocampal complex-spike and θ-neurons. *Brain Research 425*: 146-158.

Parfitt, K. D., Doze, V. A., Madison, D. V., and Browning, M. D. (1992) Isoproterenol increases the phosphorylation of the synapsins and increases synaptic transmission in dentate gyrus, but not in area CA1, of the hippocampus. *Hippocampus 2(1)*: 59-64.

Pickel, V. M., Segal, M., and Bloom, F. E. (1974) A radioautographic study of the efferent pathways of the locus coeruleus. *Journal of Comparative Neurology 155*: 15-42.

Ribak, C.E., and Seress, L. (1983) Five types of basket cell in the hippocampal dentate gyrus: a combined Golgi and electron microscopic study. *Journal of Neurology 12*: 577-597.

Robinson, T. E., Vanderwolf, C. H., and Pappas, B. A. (1977) Are the dorsal noradrenergic bundle projections from the locus coeruleus important for neocortical or hippocampal activation? *Brain Research 138*: 75-98.

Rose, G., Diamond, D., and Lynch, G. S. (1983) Dentate granule cells in the rat hippocampal formation have the behavioral characteristics of theta neurons. *Brain Research 266*: 29-37.

Rose, G. M., and Pang, K. C. H. (1989) Differential effect of norepinephrine upon granule cells and interneurons in the dentate gyrus. *Brain Research 488*: 353-356.

Sainsbury, R. S., and Partlo, L. A. (1993) Alpha$_2$ modulation of type 1 and type 2 hippocampal theta in the freely moving rat. *Brain Research Bulletin 31*: 437-442.

Scanziani, M., Gahwiler, B. H., and Thompson, S. M. (1993) Presynaptic inhibition of excitatory synaptic transmission mediated by σ adrenergic receptors in area CA3 of the rat hippocampus in vitro. *The Journal of Neuroscience 13(12)*: 5393 - 5401.

Scharfman, H. E. (1992) Differentiation of rat dentate neurons by morphology and electrophysiology in hippocampal slices: granule cells, spiny hilar cells, and aspiny 'fast spiking' cells. In: The Dentate Gyrus and Its Role in Seizures, Eds. Ribak, C. E., Gall, C. M., and Mody, I. Elsevier, New York. p. 93-109.

Segal, M., and Bloom, F. E. (1974) The action of norepinephrine in the rat hippocampus. I. Iontophoretic studies. *Brain Research 72*: 79-97.

Segal, M., and Bloom, F. E. (1974) The action of norepinephrine in the rat hippocampus. II. Activation of the input pathway. *Brain Research 72*: 99-114.

Segal, M., and Bloom, F. E. (1976) The action of norepinephrine in the rat hippocampus. III. Hippocampal cellular responses to locus coeruleus stimulation in the awake rat. *Brain Research 107*: 499-511.

Segal, M., and Bloom, F. E. (1976) The action of norepinephrine in the rat hippocampus. IV. The effects of locus coeruleus stimulation on evoked hippocampal unit activity. *Brain Research 107*: 513-525.

Seress, L., and Ribak, C. E. (1983) GABAergic cells in the dentate gyrus appear to be local circuit and projection neurons. *Experimental Brain Research 50*: 173-182. Cited by: Buzsaki, G. (1984) Feed-forward inhibition in the hippocampal formation. *Progress in Neurobiology 22*: 131-153.

Stanton. P., and Sarvey, J. M. (1985) The effect of high-frequency electrical stimulation and norepinephrine on cyclic AMP levels in normal versus norepinephrine-depleted rat hippocampal slices. *Brain Research 358*: 343-348.

Stanton, P., and Sarvey, J. M. (1985) Blockade of norepinephrine-induced long-lasting potentiation in the hippocampal dentate gyrus by an inhibitor of protein synthesis. *Brain Research 361*: 276-283.

Suzuki, S. S., and Smith, G. K. (1983) Effects of selective deafferentation and GABA-related drugs on behavior-dependent EEG spikes and neuronal bursts in normal hippocampus. *Society for Neuroscience abstracts 9*: 1105. Cited by: Buzsaki, G. (1984) Feed-forward inhibition in the hippocampal formation. *Progress in Neurobiology 22*:131-153.

Tiong, A. H. K., and Richardson, J. S. (1990) The characterization of β adrenoceptor subtypes in the rat amygdala and hippocampus. *International Journal of Neuroscience 54(3-4)*: 231-244.

Vanderwolf, C. H. (1988) Cerebral activity and behavior: control by central cholinergic and serotonergic systems. *International Review of Neurobiology 30*: 225-340.

Vanderwolf, C. H., Raithby, A., Snider, M., Cristi, C., and Tanner, C. (1993) Effects of some cholinergic agonists on neocortical slow wave activity in rats with basal forebrain lesions. *Brain Research Bulletin 31*: 515-521.

Vertes, R. P. (1980) Brain stem activation of the hippocampus: a role for the magnocellular reticular formation and the MLF. *Electroencephalography and Clinical Neurophysiology 50*: 48-58.

Woodward, D. J., Moises, H. C., Waterhouse, B. D., Hoffer, B. J., and Freedman, R. (1979) Modulatory actions of norepinephrine in the central nervous system. *Federation Proceedings. 38*: 2109-2116.

Young III, W. S., and Kuhar, M. J. (1980) Noradrenergic α1 and α2 receptors: light microscopic autoradiographic localization. *Proceedings of the National Academy of Science. USA 77(3)*: 1696-1700.